Fujisawa, J., Toita, M., Yoshida, M., 1989. A unique enhancer element for the trans activator (p40 tax) of human T-cell leukemia virus type I that is distinct from cyclic AMP-and 12-*O*-tetradecanoylphorbol-13-acetate-responsive elements. J. Virol. 63, 3234–3239.

Fujisawa, J., Toita, M., Yoshimura, T., Yoshida, M., 1991. The indirect association of human T-cell leukemia virus tax protein with DNA results in transcriptional activation. J. Virol. 65, 4525–4528.

Furukawa, Y., Yamashita, M., Usuku, K., Izumo, S., Nakagawa, M., Osame, M., 2000. Phylogenetic subgroups of human T cell lymphotropic virus (HTLV) type I in the tax gene and their association with different risks for HTLV-I-associated myelopathy/tropical spastic paraparesis. J. Infect. Dis. 182, 1343–1349.

Gessain, A., Barin, F., Vernant, J.C., Gout, O., Maurs, L., Calende, A., de The, G., 1985. Antibodies to human T-lymphotropic virus type-1 in patients with tropical spastic paraparesis. Lancet 2, 407–410.

Giraudon, P., Szymocha, R., Buart, S., Bernard, A., Cartier, L., Belin, M.F., Akaoka, H., 2000. T lymphocytes activated by persistent viral infection differentially modify the expression of metalloproteinases and their endogenous inhibitors, TIMPs, in human astrocytes: relevance to HTLV-I-induced neurological disease. J. Immunol. 164, 2718–2727.

Ikegami, M., Umehara, F., Ikegami, N., Maekawa, R., Osame, M., 2002. Selective matrix metalloproteinase inhibitor, N-biphenyl sulfonyl phenylalanine hydroxamic acid, inhibits the migration of CD4+T lymphocytes in patients with HTLV-I-associated myelopathy. J. Neuroimmunol. 127, 134–138.

Jeffery, K.J.M., Usuku, K., Hall, S.E., Matsumoto, W., Taylor, G.P., Procter, J., Bunce, M., Ogg, G.S., Welsh, K.I., Weber, J.N., Lloyd, A.L., Nowak, M.A., Nagai, M., Kodama, D., Izumo, S., Osame, M., Bangham, C.R.M., 1999. HLA alleles determine human T-lymphotropic virus-I (HTLV-I) proviral load and the risk of HTLV-I-associated myelopathy. Proc. Natl. Acad. Sci. U. S. A. 96, 3848–3853.

Jeffery, K.J.M., Siddiqui, A.A., Bunce, M., Lloyd, A.L., Vine, A.M., Witkover, A.D., Izumo, S., Usuku, K., Welsh, K.I., Osame, M., Bangham, C.R.M., 2000. The influence of HLA class I alleles and heterozygosity on the outcome of human T cell lymphotropic virus type I infection. J. Immunol. 165, 7278–7284.

Kaplan, J.E., Osame, M., Kubota, H., Igata, A., Nishitani, H., Maeda, Y., Khabbaz, R.F., Janssen, R.S., 1990. The risk of development of HTLV-I associated myelopathy/ tropical spastic paraparesis among persons infected with HTLV-I. J. Acquir. Immune Defic. Syndr. 3, 1096–1101.

Matsuoka, E., Usuku, K., Jonosono, M., Takenouchi, N., Izumo, S., Osame, M., 2000. CD44 splice variant involvement in the chronic inflammatory disease of the spinal cord: HAM/TSP. J. Neuroimmunol. 102, 1–7.

Mori, N., Sato, H., Hayashibara, T., Senba, M., Hayashi, T., Yamada, Y., Kamihira, S., Ikeda, S., Yamasaki, Y., Morikawa, S., Tomonaga, M., Geleziunas, R., Yamamoto, N., 2002. Human T-cell leukemia virus type I Tax transactivates the matrix metalloproteinase-9 gene: potential role in mediating adult T-cell leukemia invasiveness. Blood 99, 1341–1349.

Motulsky, H., 1995. Multiple Comparisons in "Intitutive Biostatistics". Oxford University Press, New York.

Nagai, M., Usuku, K., Matsumoto, W., Kodama, D., Takenouchi, N., Moritoyo, T., Hashiguchi, S., Ichinose, M., Bangham, C.R.M., Izumo, S., Osame, M., 1998. Analysis of HTLV-I proviral load in 202 HAM/TSP patients and 243 asymptomatic HTLV-I carriers: high proviral load strongly predisposes to HAM/TSP. J. Neurovirology 4, 586–593.

Nakagawa, M., Izumo, S., Ijichi, S., Kubota, R., Arimura, K., Kawabata, M., Osame, M., 1995. HTLV-I-associated myelopathy: analysis of 213 patients based on clinical and laboratory findings. J. Neurovirology 1, 50–61.

Nomoto, M., Utatsu, Y., Soejima, Y., Osame, M., 1991. Neopterin in cerebrospinal fluid: a useful marker for diagnosis of HTLV-I-associated myelopathy/tropical spastic paraparesis. Neurology 41, 457.

Nordheim, A., Rich, A., 1983. The sequence (dC-dA)n · (dG-dT)n forms left-handed Z-DNA in negatively supercoiled plasmids. Proc. Natl. Acad. Sci. U. S. A. 80, 1821–1825.

Opdenakker, G., Van Damme, J., 1994. Cytokine-regulated proteases in autoimmne diseases. Immunol. Today 15, 103–107.

Osame, M., 1990. Review of WHO Kagoshima meeting and diagnostic guidelines for HAM/TSP. In: Blattner, W.A. (Ed.), Human Retrovirology: HTLV. Raven Press, New York, pp. 191–197.

Osame, M., Usuku, K., Izumo, S., Ijichi, N., Amitani, H., Igata, A., Matsumoto, M., Tara, M., 1986. HTLV-I associated myelopathy, a new clinical entity. Lancet 1, 1031–1032.

Peters, D.G., Kassam, A., St. Jean, P.L., Yonas, H., Ferrell, R.E., 1999. Functional polymorphism in the matrix metalloproteinase-9 promoter as a potential risk factor for intracranial aneurysm. Stroke 30, 2612–2616.

Sellebjerg, F., Sorensen, T.L., 2003. Chemokines and matrix metalloproteinase-9 in leukocyte recruitment to the central nervous system. Brain Res. Bull. 61, 347–355.

Shimajiri, S., Arima, N., Tanimoto, A., Murata, Y., Hamada, T., Wang, K.Y., Sasaguri, Y., 1999. Shortened microsatellite d(CA)21 sequence down-regulates promoter activity of matrix metalloproteinase 9 gene. FEBS Lett. 455, 70–74.

Tae, H.J., Luo, X., Kim, K.H., 1994. Role of CCAAT/Enhancer-binding protein and its binding site on repression and derepression of acetyl-CoA carboxylase gene. J. Biol. Chem. 269, 10475–10484.

Tripathi, J., Brahmachari, S.K., 1991. Distribution of simple repetitive (TG/CA)n and (CT/AG)n sequences in human and rodent genomes. J. Biomol. Struct. Dyn. 9, 387–397.

Umehara, F., Izumo, S., Nakagawa, M., Ronquillo, A.T., Takahashi, K., Sato, E., Osame, M., 1993. Immunocytochemical analysis of the cellular infiltrate in the spinal cord lesions in HTLV-I-associated myelopathy. J. Neuropathol. Exp. Neurol. 52, 424–430.

Umehara, F., Okada, Y., Fujimoto, N., Abe, M., Izumo, S., Osame, M., 1998. Expression of matrix metalloproteinase and tissue inhibition of metalloproteinase in HTLV-I-associated myelopathy. J. Neuropathol. Exp. Neurol. 57, 839–849.

Vine, A.M., Witkover, A.D., Lloyd, A.L., Jeffery, K.J., Siddiqui, A., Marshall, S.E., Bunce, M., Eiraku, N., Izumo, S., Usuku, K., Osame, M., Bangham, C.R.M., 2002. Polygenic control of human T lymphotropic virus type I (HTLV-I) provirus load and the risk of HTLV-I-associated myelopathy/tropical spastic paraparesis. J. Infect. Dis. 186, 932–939.

Yu, Q., Stamenkovic, I., 1999. Localization of matrix metalloproteinase 9 to the cell surface provides a mechanism for CD44-mediated tumor invasion. Genes Dev. 13, 35–48.

Chronic progressive cervical myelopathy with HTLV-I infection

Variant form of HAM/TSP?

F. Umehara, MD; S. Nagatomo, MD; K. Yoshishige, MD; M. Saito, MD; Y. Furukawa, MD; K. Usuku, MD; and M. Osame, MD

Abstract—*Objective:* To investigate the role of human T-lymphotrophic virus type I (HTLV-I) infection in four patients who developed slowly progressive myelopathy with abnormal MRI lesions in the cervical cord levels. *Methods:* Clinical and neuroradiologic examinations were performed, and the odds that an HTLV-I-infected individual of specified genotype, age, and provirus load had HTLV-I-associated myelopathy (HAM)/tropical spastic paraparesis (TSP) were calculated. *Results:* Anti-HTLV-I antibodies were positive in both the serum and the CSF in all of the patients. Biopsied sample from spinal cord lesions showed inflammatory changes in Patient 1. Patient 2 had a demyelinating type of sensorimotor polyneuropathy. Two of the three patients examined showed high risk of developing HAM/TSP in virologic and immunologic aspects. *Conclusion:* These four cases may belong to a variant form of HAM/TSP, predominantly involving the cervical cord levels.

NEUROLOGY 2004;63:1276–1280

Human T-lymphotropic virus type I (HTLV-I) is associated with adult T-cell leukemia and a chronic progressive disease of the CNS called HTLV-I-associated myelopathy (HAM)/tropical spastic paraparesis (TSP).[1,2] The pathology of the disease involves the spinal cord, predominantly the thoracic level with atrophy of the lateral columns.[3] These lesions are associated with perivascular and parenchymal lymphocytic infiltration with the presence of foamy macrophages, proliferation of astrocytes, and fibrillary gliosis.[4]

In this article, we report four patients with slowly progressive cervical myelopathy. The calculated risk of HAM/TSP in two patients showed a high value, comparable with those of HAM/TSP and higher than those of a healthy HTLV-I carrier. Because the clinical and laboratory findings of these four cases show similarities to those of HAM/TSP, we propose that these four cases may be a variant form of HAM/TSP.

Case reports. *Patient 1.* A 56-year-old man had a year-long history of progressive gait disturbance and numbness in the upper and lower limbs. He visited a neurosurgeon, who discovered abnormal lesions in the cervical cord levels. To exclude the possibility of intramedullary spinal cord tumor, laminectomy and biopsy from the enhanced lesions were performed. Pathology revealed perivascular lymphocytic infiltration with degenerative changes of the spinal cord (figure 1). Immunohistochemical analysis revealed predominant infiltration of lymphocytes and macrophages. The patient was then referred to the Department of Neurology at the Kagoshima University Hospital.

General examinations were unremarkable. On neurologic examinations, he had normal consciousness and mentality. Cranial nerves were intact. Muscle strength in the upper and lower limbs was moderately decreased, and there was moderate muscle atrophy. Deep tendon reflexes were mildly exaggerated in the upper limbs and highly exaggerated in the lower limbs. Chaddock signs were positive bilaterally. Superficial and deep sensations were disturbed in the lower limbs. He had urinary disturbance. Anti-HTLV-I antibody was positive both in serum (×1,028) and in CSF (×64). CSF showed increased protein content (137 mg/dL), IgG level of 12.5 mg/dL, normal cell count (3/mm^3), and normal neopterin level (27 pmol/mL; normal <30 pmol/L). Myelin basic protein level was likewise normal, and there were no oligoclonal bands detected in the CSF. Western blotting of CSF for anti-HTLV-I was positive for p19, p24, p28, p53, and env. Nerve conduction studies were normal. Somatosensory evoked potentials, by stimulating the left tibial nerve, showed marked delay of central conduction time (N20: 23 milliseconds; P40: 48 milliseconds). Needle electromyography revealed fibrillation potentials in the lower limbs. Cervical MRI demonstrated swelling of the spinal cord at C5 to C6 levels with gadolinium-diethylenetriaminepentaacetate (Gd-DTPA) enhancement (figure 2). T2-weighted imaging showed high-intensity signals at the same level on sagittal section. Axial T2-weighted imaging at the C5 level showed high-intensity signals in the lateral columns bilaterally. The patient was treated with IV high-dose methylprednisolone

Additional material related to this article can be found on the *Neurology* Web site. Go to www.neurology.org and scroll down the Table of Contents for the October 12 issue to find the title link for this article.

From the Departments of Neurology and Geriatrics (Drs. Umehara, Nagatomo, Yoshishige, Saito, and Osame), Division of Blood Transfusion Medicine (Dr. Furukawa), and Department of Medical Information Science (Dr. Usuku), Graduate School of Kagoshima University, Japan.

Received February 13, 2004. Accepted in final form June 1, 2004.

Address correspondence and reprint requests to Dr. F. Umehara, Department of Neurology, Kagoshima University, Sakuragaoka 8-35-1, Kagoshima 8900075, Japan; e-mail: umehara@m2.kufm.kagoshima-u.ac.jp

Figure 1. Spinal cord pathology of Patient 1. There was massive perivascular infiltration of mononuclear cells. Hematoxylin–eosin; bar = 100 μm.

followed by oral prednisolone, but his symptoms did not improve. In the course of the following 5 years, his symptoms gradually worsened. Repeat MRI revealed atrophy of the cervical cord with high-intensity lesions at the C5 level, which may have been residual lesions of the spinal cord biopsy (figure 3). Gd-DTPA enhancement was negative.

Patient 2. A 73-year-old man noted difficulty with fine hand movements in July 2002. This gradually worsened to involve the lower extremity so that by September 2002, he could not climb a ladder. Numbness in the upper and lower limbs then developed. He also had constipation and urinary disturbance. He consulted us in November 2002. Past history was unremarkable except for blood transfusion when he was 35 years old.

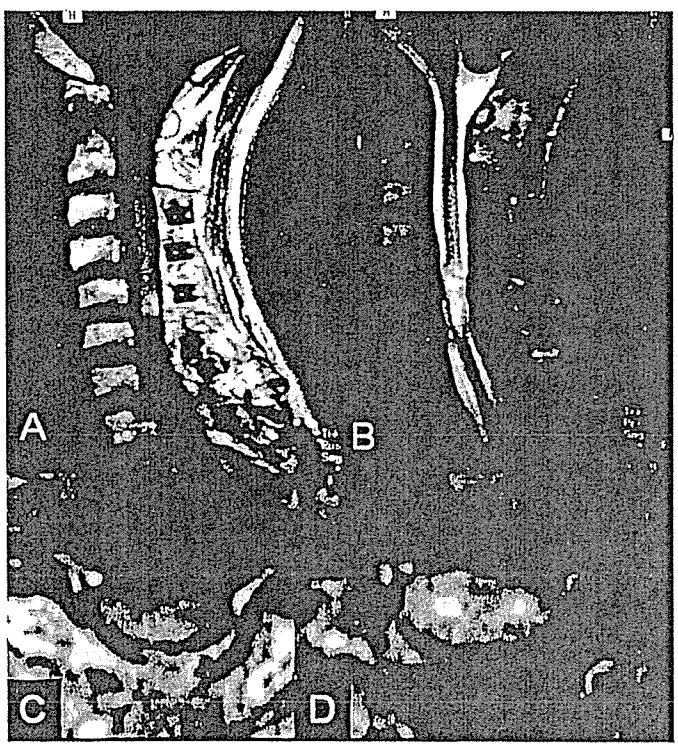

Figure 2. MRI of Patient 1, before treatment (November 1998): gadolinium-enhanced T1-weighted imaging (sagittal: A, axial: C) and T2-weighted imaging (sagittal: B, axial: D). Note spinal cord (C5 to C6) swelling with high intensity on T2-weighted imaging.

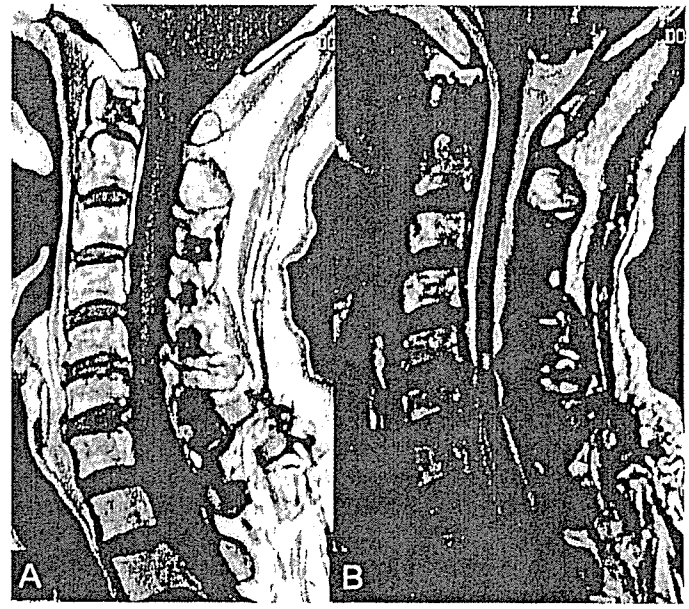

Figure 3. MRI of Patient 1: sagittal T1-weighted imaging (A) and T2-weighted imaging (B) after treatment (2003). Swelling of spinal cord with high intensity on T2-weighted imaging was markedly reduced.

General findings were likewise unremarkable. Neurologic examinations showed normal consciousness and mentality. Cranial nerves were intact. There was muscle weakness in the upper and lower limbs. Coordination in the upper limbs was poor. Deep tendon reflexes were mildly exaggerated in the upper limbs and highly exaggerated in the lower limbs. Babinski signs were positive bilaterally. Superficial sensations were decreased below the C5 level, and deep sensation was disturbed in the lower limbs. There was a tendency to fall when standing, and he was unable to walk alone. Laboratory tests were as follows: Anti-HTLV-I antibody was positive in both serum (×2,048) and CSF (×256). Western blotting of CSF for HTLV-I was positive for p19, p24, p28, p53, and env. For CSF, cell count was 10/mm^3, protein level 64 mg/dL, IgG level 9.8 mg/dL, IgG index 0.66, and neopterin level 52 pmol/mL. Nerve conduction study showed diffuse slowing of both motor and sensory nerve conduction velocity in the upper and lower limbs with prolonged F-wave latencies. Sural nerve biopsy revealed mildly decreased densities of large and small myelinated fibers. Many fibers had thinner myelin sheaths compared with their axon diameter. On teased fiber analysis, fibers with de- and remyelination (paranodal demyelination: 7%, segmental demyelination: 5%, segmental remyelination: 20%) and axonal degeneration (5%) increased. Cervical MRI revealed swelling of the spinal cord without Gd-DTPA enhancement (see figure E-1 on the *Neurology* Web site at www.neurology.org). T2-weighted imaging showed high-intensity lesions from the C3 to C7 levels, which were located mainly in the posterior and lateral columns bilaterally. High-dose methylprednisolone (1,000 mg/day for 3 days) followed by oral prednisolone treatment gradually improved his muscle weakness in the upper and lower limbs with disappear-

ance of both high-intensity lesions and swelling of the cervical cord levels. One and one-half years after the treatment, MRI revealed spinal cord atrophy mainly at the middle thoracic levels without abnormal intensity.

Patient 3. In January 2003, a 51-year-old woman noticed difficulty in walking, which gradually worsened in the following months. She visited us in April 2003. She had been experiencing pemphigus vulgaris since age 17. General examinations revealed whole-body skin eruption. Neurologic examinations showed normal consciousness and mentality. Cranial nerves were intact. There was resting and postural tremor of both hands. Muscle strength in the upper limbs was normal but was mildly reduced in the lower limbs. Deep tendon reflexes were mildly exaggerated in the upper limbs and highly exaggerated in the lower limbs. Babinski signs were positive bilaterally. Superficial sensations were decreased in the distal parts of the lower limbs, and deep sensation was markedly disturbed in the lower limb. She was unable to stand. Laboratory tests as follows: Anti-HTLV-I antibody was positive in both serum (×8,192) and CSF (×512). Serum deoxytimidine kinase activity was 73.4 U/L (<5.0). For CSF, cell count was 26/mm^3, protein level 96 mg/dL, glucose level 45 mg/dL, and IgG index 0.99. Oligoclonal bands were positive. Nerve conduction studies were unremarkable. Cervical MRI revealed swelling of the spinal cord without Gd-DTPA enhancement (see figure E-2 on the *Neurology* Web site). T2-weighted imaging showed high-intensity lesions from the C3 to T3 levels, which were located mainly in the posterior columns bilaterally. High-dose methylprednisolone (1,000 mg/day for 3 days) followed by oral prednisolone treatment gradually improved her lower limb weakness. Both high-intensity lesions and swelling of the cervical cord levels decreased. During the following 6 months, her symptoms gradually improved.

Patient 4. In November 1998, a 68-year-old man noticed difficulty in walking, which gradually worsened. In February 1999, he was diagnosed as having lumbar canal stenosis and underwent laminectomy of the fourth lumbar vertebrae. Numbness and pain below the level of the navel developed 2 weeks after the operation. He also noticed constipation and urinary disturbance. He visited us in June 1999. He had cerebral infarction and had had angina pectoris since 1993. General findings were unremarkable. Neurologic examinations showed normal consciousness and mentality. Cranial nerves were intact. Muscle strength was mildly reduced in the upper limbs and markedly reduced in the lower limbs. Deep tendon reflexes were mildly exaggerated in the upper limbs and highly exaggerated in the lower limbs. Babinski signs were positive bilaterally. Superficial sensations were decreased below the T3 level, and deep sensation was disturbed in the lower limbs. He was unable to stand. Laboratory tests are as follows: Anti-HTLV-I antibody was positive in both serum (×4,096) and CSF (×32). For CSF, cell count was 2/mm^3, protein level 167 mg/dL, IgG level 29 mg/dL, IgG index 0.66, and neopterin level 52 pmol/mL. Nerve conduction studies were unremarkable. Cervical MRI revealed swelling of the spinal cord without Gd-DTPA enhancement (see figure E-3 on the *Neurology* Web site). T2-weighted imaging showed high-intensity lesions from the C2 to T5 levels, which were located mainly in the posterior and lateral columns bilaterally. High-dose methylprednisolone (1,000 mg/day for 3 days) followed by oral prednisolone and cyclophosphamide pulse therapy (1,000 mg/day for 1 day) gradually improved his muscle weakness in all four limbs. There was also decrease of both high-intensity lesions and swelling of the cervical cord levels. During the following 4 years, his symptoms remained stable.

Materials and methods. *Evaluation of risk of HAM/TSP.* We calculated the odds that an HTLV-I-infected individual living in Kagoshima prefecture, of specified genotype, age, and provirus load, had HAM/TSP by an equation specifically developed for this population.[5] As all four patients in this report live in Kagoshima prefecture, blood samples from Patients 1 to 3 were analyzed upon obtaining informed consent. For the control subjects, we used the study cohort, which consisted of 52 patients with HAM/TSP attending the Department of Neurology and Geriatrics, Kagoshima University (Kagoshima, Japan), and 47 healthy carriers (HCs) of HTLV-I randomly selected from the same geographic location, as described elsewhere.[6,7] All individuals screened were of Japanese descent and resided within Kagoshima prefecture (Kyushu, Japan). The diagnosis of HAM/TSP was made in accordance with World Health Organization criteria.[8] Peripheral blood was obtained from all individuals upon obtaining of informed consent. Fresh peripheral blood mononuclear cells (PBMCs) were obtained by density gradient centrifugation using a Histopaque-1077 instrument (Sigma, Tokyo, Japan) and washed three times with phosphate-buffered saline containing 1% fetal calf serum. Isolated PBMCs were cryopreserved in liquid nitrogen until use. Genomic DNA was extracted from PMBCs using a QIAamp blood kit (Qiagen, Tokyo, Japan) according to the manufacturer's instructions.

Genotyping methods for non–human leukocyte antigen candidate genes. For each candidate gene, we went on to do genotyping either by DNA sequencing or by PCR with allele-specific primers as previously described.[6]

Human leukocyte antigen typing. The results of the molecular genotyping of class I and class II human leukocyte antigen (HLA) loci in this cohort have been reported elsewhere.[6,7]

HTLV-I genotyping. Two subgroups (A and B) of the cosmopolitan genotype of HTLV-I are present in Kagoshima, Japan. Molecular typing of the HTLV-I *tax* gene was done as described elsewhere to identify the HTLV-I subgroup present in each infected subject.[9]

Provirus load measurement. The provirus load in PBMCs was measured using real-time PCR with an ABI 7700 sequence detection system (Applied Biosystems, Foster City, CA). With use of β-actin as an internal control, the amount of HTLV-I proviral DNA was calculated by the following formula: copy number of HTLV-I (pX) per 1×10^4 PBMCs = ([copy number of pX]/[copy number of β-actin/2]) $\times 10^4$. All samples were performed in triplicate. All samples were amplified and analyzed in triplicate, as described elsewhere.[10]

Odds of developing HAM/TSP. We calculated the odds that an HTLV-I-infected individual of specified genotype, age, and provirus load had HAM/TSP by using the equation based on the logistic regression analysis in the Kagoshima cohort as previously described.[6] A worked example is as follows: HTLV-I-infected individual in Kagoshima, 60 years old, with a $\log_{10}$ (provirus load) of 2.5 with the genotype *TNF -863A*$^+$, *SDF-1 + 801AA*, *HLA-A*02*$^-$, *HLA-Cw*08*$^+$, HTLV-I subgroup B has a predicted n odds of HAM/TSP of $-1.716 - (0.145 \times 60) + (0.003 \times 60^2) + (0.46 \times 2.5) + (0.487 \times 2.5^2) + 3.057 - (4.616 \times 2.5) + (1.476 \times 2.5^2) - 1.689 - 0.894 - 1.587 = 1.864$. That is, this HTLV-I-infected individual's odds of developing HAM/TSP is equal to $\exp(-1.864) = 0.155$.

Results. The results are summarized in the table and in figure 4. Among the patients with HAM/TSP and HC, 39 cases showed odds above 3.0. In these 39 cases, 37 cases (95%) had HAM/TSP, and only 2 cases (5%) were HCs. Except for Patient 3, the odds for HAM/TSP in Patients 1 and 2 were comparable with those of HAM/TSP, higher than those of an HC.

Discussion. The four patients had several features in common: 1) progressive cervical myelopathy with

Table Analysis of risk factors for developing HAM/TSP

Patient no.	Sex	ln odds of HAM	Odds of HAM	Age, y	*tax**	Log_{10} *tax*	*HLA*-DR1*	*HLA*-A02*	*HLA*-Cw08*	Genotype *TNF-α*	Genotype *SDF-1*	Genotype *IL-10*	HTLV-I subgroup
1	M	2.30	9.9	56	344	2.54	+	−	−	CC	GG	AC	B
2	M	3.40	29.9	73	198	2.30	−	−	+	AC	AA	AC	B
3	F	−1.20	0.3	51	128	2.11	−	+	−	CC	GA	AC	B

* Amount of human T-lymphotropic virus type I (HTLV-I) proviral DNA/10^4 peripheral blood mononuclear cells.
HAM/TSP = HTLV-I-associated myelopathy/tropical spastic paraparesis.

a duration of several months to years, 2) abnormal lesions in the cervical to upper thoracic cord levels with or without Gd-DTPA enhancement, 3) anti-HTLV-I antibodies positive in both serum and CSF, and 4) high levels of HTLV-I proviral load in PBMCs. We screened for other causes of myelopathy including neurosarcoidosis, parasitic myelitis, multiple sclerosis, atopic myelitis, and Sjögren syndrome, but these diseases were unlikely in any of the four cases. We then suspected that these cases might be associated with HTLV-I infection.

The most striking difference from the typical HAM/TSP is the presence of abnormal MRI lesions in the cervical cord. There was swelling of the spinal cords with high-intensity lesions, which were located mainly in bilateral posterior columns, posterior horns, or lateral columns. In Case 1, biopsy samples revealed massive lymphocytic perivascular infiltration in the parenchyma. In Cases 2, 3, and 4, abnormal MRI findings in the cervical cord diminished after corticosteroid treatment or long-term follow-up. These findings suggest that the abnormal cervical MRI lesions may be inflammatory in nature. This is in contrast to the ordinary type of HAM/TSP, the hallmark finding being because spinal cord atrophy predominantly involves the thoracic cord levels without Gd-DTPA enhancement. Recently, atypical MRI findings have been reported in patients with HAM/TSP. In two of the cases, T2-weighted imaging showed high signal intensity lesions from the cervical to the thoracic cord levels with Gd-DTPA enhancement.[11] The other two cases of HAM patients revealed swelling of the spinal cord with Gd-DTPA enhancement and faint high T2 signal intensities.[12,13] This is not at all surprising because there is usually intense perivascular inflammation with destruction of the blood–brain barrier in actively inflamed lesions of the spinal cord.[3,4] Neuropathology of spinal cord biopsy specimens from Gd-enhanced spinal cord lesions in a patient with HAM/TSP demonstrated infiltration of the leptomeninges and adjacent spinal cord parenchyma by numerous mononuclear cells.[14] Thus, abnormal MRI lesions in the current four cases are not incompatible with HAM/TSP.

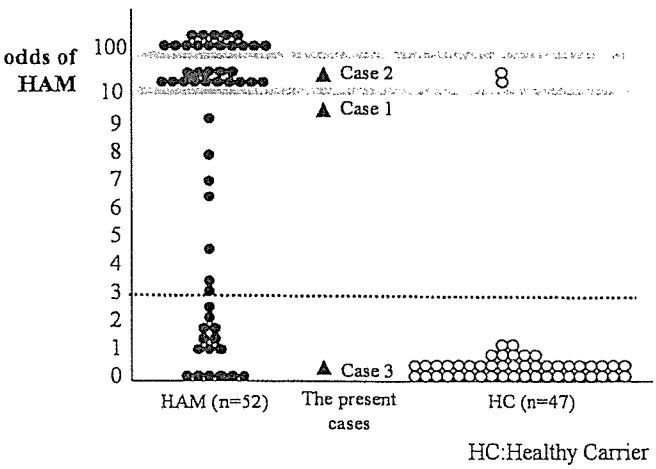

Figure 4. Odds of developing human T-lymphotropic virus type I–associated myelopathy (HAM)/tropical spastic paresis (TSP). Note Patients 1 and 2 showed high odds of developing HAM/TSP.

In Case 2, a demyelinating polyneuropathy complicated his condition. Complications of peripheral neuropathy have been reported in patients with HAM/TSP,[15] and sural nerve pathology of patients with peripheral neuropathy and HAM/TSP showed nonspecific changes including both chronic demyelinating changes and axonal loss. Thus, the polyneuropathy in Case 2 may be associated with HTLV-I infection.

To further confirm the role of HTLV-I infection in these cases, we calculated the risk of developing HAM/TSP by the best-fit logistic regression equation for the risk of HAM/TSP in the Kagoshima HTLV-I-infected cohort.[6] This equation allowed for the correct identification of 88% of cases of HAM/TSP. The algorithm, however, can be justifiably used to calculate the odds of HAM/TSP only in a Kagoshima cohort and may not be applicable to another population. Our results confirmed that individuals having odds of >3.0 have a high risk of developing HAM/TSP. Taking this into consideration, Patients 1 and 2 had comparably high risks of developing HAM/TSP. Therefore, HTLV-I infection may not only be coincidental but could be closely associated with the neurologic disorders in these patients.

Acknowledgment

The authors thank Dr. Arlene R. Ng for critical reading of the manuscript.

References

1. Osame M, Matsumoto M, Usuku K, et al. Chronic progressive myelopathy associated with elevated antibodies to human T-lymphotropic type I and adult T cell leukemia-like cells. Ann Neurol 1987;21:117–122.
2. Gessain A, Barin F, Vernant JC, et al. Antibodies to human T-lymphotropic virus type-I in patients with tropical spastic paraparesis. Lancet 1985;2:407–410.

3. Iwasaki Y. Pathology of chronic myelopathy associated with HTLV-I infection (HAM/TSP). J Neurol Sci 1990;96:103–123.
4. Umehara F, Osame M. Histological analysis of HAM/TSP pathogenesis. In: Sugamura K, Uchiyama T, Masao M, Kannagi M, eds. Two decades of adult T-cell leukemia and HTLV-I research. Tokyo: Japan Scientific Societies Press, 2003:141–148.
5. Vine AM, Witkover AD, Lloyd AL, et al. Polygenic control of human T lymphotropic virus type I (HTLV-I) provirus load and the risk of HTLV-I-associated myelopathy/tropical spastic paraparesis. J Infect Dis 2002; 186:932–939.
6. Jeffery KJ, Usuku K, Hall SE, et al. HLA alleles determine human T-lymphotropic virus-I (HTLV-I) proviral load and the risk of HTLV-I-associated myelopathy. Proc Natl Acad Sci USA 1999;96:3848–3853.
7. Jeffery KJ, Siddiqui AA, Bunce M, et al. The influence of HLA class I alleles and heterozygosity on the outcome of human T cell lymphotropic virus type I infection. J Immunol 2000;165:7278–7284.
8. Osame M. Review of WHO Kagoshima meeting and diagnostic guidelines for HAM/TSP. In: Blattner WA, ed. Human retrovirology: HTLV. New York: Raven Press, 1990:191–197.
9. Furukawa Y, Yamashita M, Usuku K, et al. Phylogenetic subgroups of human T cell lymphotropic virus (HTLV) type I in the tax gene and their association with different risks for HTLV-I-associated myelopathy/tropical spastic paraparesis. J Infect Dis 2000;182:1343–1349.
10. Nagai M, Usuku K, Matsumoto W, et al. Analysis of HTLV-I proviral load in 202 HAM/TSP patients and 243 asymptomatic HTLV-I carriers: high proviral load strongly predisposes to HAM/TSP. J Neurovirol 1998;4:586–593.
11. Tajima Y, Kishimoto R, Sudoh K, et al. Spinal magnetic resonance image alterations in human T-lymphotropic virus type I-associated myelopathy patients before and after immunomodulating treatment. J Neurol 2003;250:750–753.
12. Shakudo M, Inoue Y, Tukada T. HTLV-I-associated myelopathy: acute progression and atypical MR findings. AJNR Am J Neuroradiol 1999; 20:1417–1421.
13. Watanabe M, Yamashita T, Hara A, et al. High signal intensity in the spinal cord on T2-weighted images in rapidly progressive tropical spastic paresis. Neuroradiology 2001;43:231–233.
14. Levin MC, Lehky TJ, Fierlage AN, et al. Immunologic analysis of a spinal cord-biopsy specimen from a patient with human T-cell lymphotropic virus type I-associated neurologic disease. N Engl J Med 1997;336:839–844.
15. Kiwaki T, Umehara F, Arimura Y, et al. The clinical and pathological features of peripheral neuropathy accompanied with HTLV-I associated myelopathy. J Neurol Sci 2003;206:17–21.

AIDS RESEARCH AND HUMAN RETROVIRUSES
Volume 20, Number 10, 2004, pp. 1092–1099

Human T Cell Lymphotropic Virus Type I (HTLV-I) $p12^I$ Is Dispensable for HTLV-I Transmission and Maintenance of Infection *in Vivo*

YOSHITAKA FURUKAWA,[1] KOICHIRO USUKU,[2] SHUJI IZUMO,[3] and MITSUHIRO OSAME[4]

ABSTRACT

The function of the $p12^I$ protein of human T cell lymphotropic virus type I (HTLV-I) has been under debate. p12K (lysine) and p12R (arginine) variants of this protein at amino acid 88 and a shorter life of p12K had been reported by another group. Because HTLV-I-associated myelopathy/tropical spastic paraparesis (HAM/TSP) patients usually have a higher provirus load than asymptomatic HTLV-I carriers (ACs), and $p12^I$ had been suggested to confer a proliferative effect on HTLV-I-infected cells *in vitro*, it is possible that the relatively unstable p12K is less frequent in HAM/TSP patients than in ACs. To elucidate whether p12K and other alterations in the *p12* gene were related to the outcome of HTLV-I infection, we sequenced the *p12* gene in 144 HAM/TSP patients, 41 adult T cell leukemia (ATL) patients, and in 46 ACs. p12K was observed in only two HAM/TSP patients, but was not present in either ATL patients or ACs. Interestingly, a premature termination codon in the *p12* was observed in 5.6% of HAM/TSP patients and in 4.9% of ATL patients but none was found in ACs. The *p12* initiation codon was destroyed in one HAM/TSP patient. These HTLV-I variants with truncated p12 protein or with a destroyed initiation codon in the *p12* gene appeared to have been transmitted in the subjects' families. These findings suggest that *p12* is dispensable for the transmission and maintenance of HTLV-I infection, although it is premature to conclude that sequence varitation in the *p12* gene is associated with differences in the outcome of HTLV-I infection.

INTRODUCTION

HUMAN T CELL LYMPHOTROPIC VIRUS TYPE I (HTLV-I) was first isolated from a cutaneous T-lymphoma in 1980,[1] and was determined to be the etiological agent of adult T cell leukemia (ATL).[2] In 1985 an association was reported between tropical spastic paraparesis, which had been considered to be a degenerative disorder, and HTLV-I.[3] In 1986 HTLV-I was reported to be associated with a similar syndrome, which was called HTLV-I-associated myelopathy (HAM);[4] the condition is now called HAM/TSP. One of the intriguing questions associated with HTLV-I infection is why the same HTLV-I causes two distinct diseases. Another question is why only a small proportion of infected people, approximately 2–3%, develop ATL,[5] and a further 0.25% develop HAM/TSP in Japan,[6] while the majority (about 97%) of HTLV-I-infected individuals develop no associated disease. To date, HTLV-I provirus isolated from ATL and HAM/TSP patients was reported to be indistinguishable in the LTR and env regions.[7] However, we recently reported the existence of subgroups in the *tax* gene and different risks of HAM/TSP among different HTLV-I subgroups.[8] Tax is a multifunctional protein encoded by the open reading frame IV of the pX region of HTLV-I that can transactivate HTLV-I transcription through LTR.[9] Tax can also transactivate many

[1]Division of Blood Transfusion Medicine and Cell Therapy, Kagoshima University Hospital, 8–35–1 Sakuragaoka, Kagoshima 890–8520, Japan.
[2]Department of Medical Informatics, Faculty of Medicine, Kagoshima University, Kagoshima, Japan.
[3]Center for Chronic Viral Diseases, Faculty of Medicine, Kagoshima University, Kagoshima, Japan.
[4]Department of Neurology and Geriatrics, Kagoshima University Graduate School of Medical and Dental Science, Kagoshima, Japan.

cytokine genes[10,11] and protooncogenes.[12] These observations raise the interesting possibility that differences in Tax may influence the outcome of HTLV-I infection. $p12^I$ is another protein encoded by the open reading frame I of the pX region, the function of which is not well elucidated.[13] The $p12^I$ protein can bind to the 16-kDa subunit of the H^+-ATPase proton pump[14] and to the β and γc chains of the interleukin 2 (IL-2) receptor.[15] Although $p12^I$ does not influence the infectivity of HTLV-I in *in vitro* culture, it has been suggested that $p12^I$ is necessary for persistent HTLV-I infection in the rabbit model.[16] When $p12^I$ was expressed under experimental conditions, $p12^I$ was reported to reside in the endoplasmic reticulum and Golgi,[17] and to be associated with several proteins such as calcium-binding protein,[18] and free major histocompatibility complex class I heavy chain (MHC-I-Hc).[19] Association of $p12^I$ with calreticulin modulates activation of nuclear factor of activated T cells, and enhances STAT5 activation.[20] Binding of the $p12^I$ with MHC-I-HC was shown to result in a significant decrease in the surface level of MHC-I on human T cells.[19] These previously reported findings suggested that $p12^I$ might confer a proliferative advantage on HTLV-I-infected cells and also may affect the result of HTLV-I infection.

The $p12^I$ protein with lysine in the C-terminal region (position 88: p12K) was shown to be a substrate for ubiquitylation and degradation by the proteasome. Also, the p12K variant has a half-life significantly shorter than that of $p12^I$ with arginine in the same position (p12R).[21] There have been conflicting results concerning the prevalence of these p12K and p12R alleles in HAM/TSP patients and asymptomatic carriers (ACs). p12K was reported to be more frequent in HAM/TSP patients than in ACs in one study.[21] Another study reported that p12K was observed in a small minority of both HAM/TSP patients and ACs.[22] Although it had been suggested that $p12^I$ confers a proliferative advantage of HTLV-I-infected cells *in vitro*, the effect of $p12^I$ *in vivo*, if it is indeed expressed, may be different. If p12K, which is more unstable than p12R, is more frequently observed in HAM/TSP patients (who usually have a higher HTLV-I provirus load) than in ACs, one possibility is that a shorter life of p12K is associated with greater proliferation of HTLV-I-infected cells *in vivo*. We therefore set out to examine whether the p12K variant is present at a significantly higher frequency in HAM/TSP patients than in ACs in Japan, and whether the p12R/K allele was associated with the HTLV-I tax viral genotype, that we previously reported influenced the risk of HAM/TSP development in this Japanese population. We then extended our study to examine other variations in the *p12* gene, to test whether $p12^I$ is dispensable for HTLV-I infection in humans, and whether variations in the *p12* gene were associated with different risks of HTLV-I-associated diseases. We discuss the role of $p12^I$ in the establishment of stable infection in humans, and the association between sequence variations in the *p12* gene of HTLV-I and HTLV-I-related diseases.

MATERIALS AND METHODS

Study population

One hundred and forty-four cases of HAM/TSP were compared with 41 ATL patients (30 acute type, 3 lymphoma type, 6 chronic type, and 2 smoldering type ATL) and 46 randomly selected HTLV-I-seropositive asymptomatic blood donors (ACs). All cases and controls were of Japanese ethnic origin and resided in Kagoshima prefecture, Japan. The diagnosis of HAM/TSP was made according to the World Health Organization diagnostic criteria.[23] The diagnosis and clinical subtype of ATL were made according to Shimoyama's criteria.[24] Asymptomatic carriers were randomly selected from 111 individuals who were notified by the Red Cross following blood donation that they were infected with HTLV-I and subsequently attended our clinic.[25]

Sequencing of HTLV-I p12 gene

All DNA samples extracted from peripheral blood mononuclear cells (PBMCs) were sequenced from position 6801–7199 (numbered as in the reference strain ATK),[26] which included the entire HTLV-I *p12* gene (nucleotides 6834–7130). Polymerase chain reaction (PCR) was done on the extracted DNA to amplify proviral DNA, and nucleotide sequences were determined in both directions. One hundred nanograms of DNA was amplified by 35 cycles of PCR using Expand high fidelity PCR system (Boehringer Mannheim, Japan) and 1 μM primers [ORFI03$^+$: 5′-CGTCAGATACCCCCATTACTC-3′ (6598–6619) and ORFI02$^-$: 5′-AGCCGATAACGCGTCCATCGAT-3′ (7472–7493)]. Each PCR cycle consisted of denaturation at 94°C for 60 sec, annealing at 58°C for 75 sec, extension at 72°C for 90 sec, and extension of the final cycle at 72°C for 10 min. Amplified DNA products were purified using the QIA quick purification kit (Qiagen, Japan) and 0.1 μg of PCR products was sequenced using the dye terminator DNA sequencing kit (Applied Biosystems, Japan) with 3.2 pmol of each primer (ORFI03$^+$, ORFI02$^-$) in an automatic sequencer (377 DNA Sequencer, Applied Biosystems).

Restriction fragment length polymorphism analysis of HTLV-I tax

Subgroup analysis of the Japanese HTLV-I *tax* genes was performed as described elsewhere.[8] Substitution at nucleotide position 8344 of the *tax* gene creates an AccII restriction site. One microliter of the first PCR product of the *tax* gene amplified with primers PXO1$^+$ and PXO2$^-$ was subjected to a further 20 cycles of PCR with primers PXI3$^+$ and PXI3$^-$. Two microliters of the nested PCR product was digested with 5 U of *Acc*II (Takara, Japan) in a 10 μl reaction volume at 37°C for 1 hr and the product was electrophoresed on a 1% agarose gel. When the PCR product was cut by *Acc*II, the sample was identified as *tax* A, and when uncut, the sample was identified as *tax* B.

Proviral load measurement

The HTLV-I provirus load in PBMC was measured in HAM/TSP patients and ACs as described.[27] A quantitative PCR reaction was performed using the ABI PRISM 7700 sequence detector (Perkin-Elmer Applied Biosystems). The amount of HTLV-I proviral DNA was calculated as follows: copy number of HTLV-I (*tax*) per 10^4 PBMC = [copy number of *tax*/(copy number of β-actin/2)] $\times$ 10^4. The lower limit of detection was 1 copy per 10^4 PBMC.

RESULTS

Existence of p12K variant at low frequency in HAM/TSP patients

We analyzed 231 samples from 144 HAM/TSP patients, 41 ATL patients, and 46 ACs, all of them residing in Kagoshima, southern Japan. The grand consensus sequence of these 231 samples differed from the reference ATK strain at nucleotide position 6906 (A to G; leading to the amino acid change from serine in ATK to glycine in the grand consensus sequence), 6984 and 6985 (G to A in both positions; leading to the amino acid change from glycine in ATK to asparagine in the grand consensus sequence). There were HTLV-I subgroup-specific nucleotides at nucleotide positions 6900 and 6905. The nucleotide at position 6900 was T and the corresponding amino acid was serine in all of the HTLV-I sequences with *tax* A (31 cases in this study); this nucleotide was C and the amino acid was proline in all of the HTLV-I with *tax* B (200 cases in this study). The nucleotide at position 6905 was G in all HTLV-I sequences with *tax* A (31 cases in this study); in *tax* B this nucleotide was T but this difference does not correspond to an amino acid alteration. In Figure 1, we summarize the observed nucleotide alterations and amino acid changes that were not specific to an HTLV-I subgroup. In Table 1, we summarize amino acid changes that may influence the function of $p12^I$. The p12K variant was observed only in HAM/TSP patients; however, it was present at a low frequency (2 out of 144; 1.39%). All other samples, including HAM/TSP, ATL, and AC's had the p12R variant. One of the p12K subjects was a 65-year-old female who had had HAM/TSP for 8 years; the other was a 72-year-old female who had had HAM/TSP for 22 years. In each of these subjects, the *tax* subgroup was *tax* B. Serum anti-HTLV-I antibody titer and HTLV-I provirus load are summarized in Table 2. The HTLV-I provirus load tended to be lower in these two subjects, although a meaningful statistical analysis was not applicable because of the small number.

Premature stop codon preceding the p12R/K allele, alteration of initiation codon in p12 and other alteration

Interestingly, in 7 out of 144 HAM/TSP patients, a nucleotide substitution from G to A at nt positions 7087 (one patient) or 7088 (six patients) created a premature stop codon just upstream of the p12R/K allele (amino acid at position 87 of the $p12^I$ protein was changed from W to Stop). In another HAM/TSP patient, a nucleotide substitution from G to A at nt position 7078 also created a premature stop codon five amino acids upstream of the p12R/K allele (amino acid at position 82 of the p12 protein was changed from W to Stop). In one other HAM/TSP patient, nucleotide substitutions from T to C at nt 7086 and from G to A at nt 7088 were observed simultaneously, resulting in an amino acid substitution from W to R, one amino acid upstream of the p12R/K allele. In one other HAM/TSP patient, a nucleotide substitution from G to A at nt position 6836 destroyed the initiation codon of p12 (M to I). In ATL cases, there were two patients with a premature stop codon just upstream of the p12R/K allele out of 41 patients. However, in ACs, there was no subject with a premature stop codon in the *p12* gene. Ages and other laboratory findings are summarized in Table 2. There was an ATL specific nucleotide alteration at nt position 6909 in 3 out of 41 ATL patients (Fig. 1B), which was the most frequently observed alteration. The nucleotide alteration from G to A at this position changed the amino acid from aspartate to asparagine.

HTLV-I subgroup-specific nucleotide alteration, p12R/K allele, and the premature stop codon in p12 are stable over time (Table 3)

To examine if subgroup-specific nucleotide alterations, the p12R/K allele, and the premature stop codon were stable over time, we sequenced the HTLV-I p12 gene at different time points in cases with these nucleotide alterations. The nucleotide at position 6900 was T in HTLV-I sequences with *tax* A and this residue was C in HTLV-I with *tax* B. The nucleotide at position 6905 was G in HTLV-I sequences with *tax* A and this residue was T in HTLV-I with *tax* B. These nucleotide alterations existed stably for 7 years in the HAM 70 case (Table 3). The p12R allele existed stably for 7 years in the HAM 57 case. Also, the p12K allele existed stably for 9 years in the HAM 79 case (Table 3). The premature stop codon in the *p12* gene was also stably maintained in HAM 105 and in HAM 181 for 9 years in both cases (Table 3). No case was found in which these sequence variants changed over time in one individual.

HTLV-I with premature stop codon in p12 gene is transmissible (Table 4)

To examine whether HTLV-I with a premature stop codon in the *p12* gene is transmissible, we sequenced the *p12* gene in asymptomatic carriers who are family members of cases with a premature stop codon in the *p12* gene. HTLV-I carriers who are family members of three HAM/TSP patients with a *p12* premature stop codon were examined. Each family member had a sequence of the *p12* gene that was identical to that of the HAM/TSP patients in their respective family. For example, the husband of HAM 181 had an identical *p12* sequence with substitution at 7078, which created a stop codon that was observed only in this family. The wife of HAM 201 had an identical *p12* gene sequence with substitutions at 6840, 7094 (creating a stop codon), and 7134, in addition to the HTLV-I subgroup-specific substitutions at 6900 and 6905. A sister and the mother of HAM 790 had an identical *p12* gene sequence with the stop codon at nucleotide 7094.

HTLV-I with destroyed initiation codon in the p12 gene was also transmitted (Table 4)

To examine whether HTLV-I with a destroyed initiation codon in the *p12* gene was also transmitted, we checked family members of patient HAM 271 who carried an HTLV-I provirus with a destroyed initiation codon. Samples from two sisters of this patient were available, one of whom was previously diagnosed as HAM/TSP. The p12 sequence was identical, with a destroyed initiation codon of *p12*, among these three sisters.

DISCUSSION

Recently, the function of the $p12^I$ of HTLV-I has been under debate, and natural variants of *p12* at position 88 (arginine,

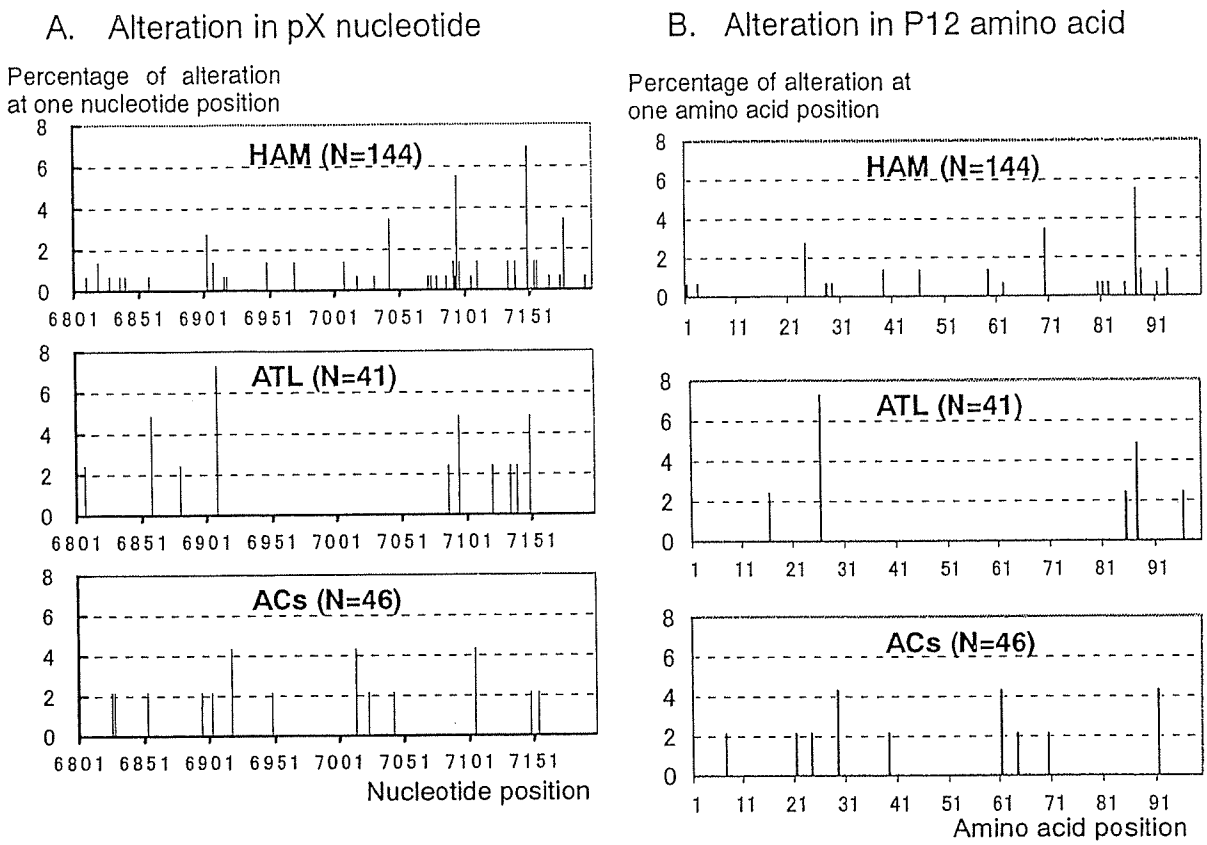

FIG. 1. Summary of the nucleotide and amino acid alterations. (A) Summary of the nucleotide alterations in pX that covers the p12[I] protein. Upper column: HAM/TSP patients. Middle column: ATL patients. Lower column: Asymptomatic carriers. *x*-axis, nucleotide position. *y*-axis, percentage of nucleotide alteration at one nucleotide position. (B) Summary of the amino acid alterations in the p12[I] protein. Upper column: HAM/TSP patients. Middle column: ATL patients. Lower column: Asymptomatic carriers. *x*-axis, amino acid position of the p12[I] protein. *Y*-axis, percentage of the amino acid alteration at one amino acid position.

p12R and lysine, p12K) were reported.[21] Lysine at position 88 in p12[I] is a ubiquitylation site and a shorter life of p12K compared to p12R was reported. p12K was previously reported to be frequent and specific in HAM/TSP patients,[21] but there was also a conflicting report.[22] The main purpose of the present study was to elucidate if variations in the *p12* gene were associated with HTLV-I related diseases, especially with respect to the distribution of p12 R/K variation in HAM/TSP, ATL, and ACs. We also examined whether the p12R/K variation was associated with the HTLV-I *tax* viral genotype, which we previously reported to influence the risk of HAM/TSP development.[8]

The p12K variant was observed in only two HAM/TSP pa-

TABLE 1. SUMMARY OF AMINO ACID CHANGES IN p12[I] PROTEIN THAT MAY INFLUENCE THE FUNCTION[a]

Amino acid position (change in amino acid)	*HAM/TSP (N = 144)*	*ATL (N = 41)*	*ACs (N = 46)*
1 (M to I)	1 (0.7%)	0	0
82 (W to Stop)	1 (0.7%)	0	0
87 (W to Stop)	7 (4.9%)	2 (4.9%)	0
88 (R to K)	2 (1.4%)	0	0
Total	11 (7.6%)	2 (4.9%)	0

[a]Number of cases that have amino acid change at the position described in the left column is stated. Amino acid change of p12[I] is shown in parentheses in the left column. Percentage of cases are shown in parentheses in the HAM/TSP, ATL, and ACs columns.

TABLE 2. CHARACTERIZATION OF HAM/TSP PATIENTS WITH DESTROYED INITIATION CODON, PREMATURE STOP CODON, AND p12R/K ALLELE IN THE p12 GENE

Amino acid position (change in amino acid)	*No. of cases*	*Age*	*Anti-HTLV-I antibody[a] (PA)*	*HTLV-I provirus load[a]*
1 (M to I)	1	43	8192	1954
82 (W to Stop)	1	63	32768	1343
87 (W to Stop)	7	41[b]	8192	641
88 (R to K)	2	69[b]	9216	146
All HAM/TSP patients	144	56[b]	8192	586

[a]Anti-HTLV-I antibody titer and HTLV-I provirus load are stated as median value.
[b]Mean age is shown.

tients but did not occur either in ATL patients or in ACs. However, the frequency of p12K was very low (2 out of 144; 1.4%). Regarding the association of p12R/K alleles and the *tax* subgroup, two HTLV-I-seropositive subjects with p12K were classified to have *tax* B. However, another HTLV-I-seropositive individual with *tax* B (119 HAM patients) had p12R. Also, of the 142 HAM/TSP patients who carried p12R, 23 HAM/TSP patients had *tax* A and 119 had *tax* B. Trovato also reported that p12R/K alleles were found regardless of the geographical origin.[21] These findings suggest that the p12R/K variation is not specifically associated with the HTLV-I subgroup. Also, the very low frequency of the p12K variant observed among HAM/TSP patients in Japan cannot be explained by the particular distribution of the HTLV-I subgroup in Japan: most of the HTLV-I in Japan belongs to Cosmopolitan B, while Cosmopolitan A is widely distributed through the world.

Although the p12K variant, which may have a decreased biological effect because of its shorter life, was found at a very low frequency in HAM/TSP patients, other variations in the *p12* gene that can affect the function of *p12* were found in HAM/TSP and in ATL patients. A premature stop codon was found in eight HAM/TSP patients and in two ATL patients but not in ACs. Trovato *et al.*[21] also reported this termination codon immediately preceding the lysine in one ATL patient who also had HAM/TSP. Because the $p12^{I}$ sequence with a premature stop codon immediately preceding the p12R/K allele had arginine in our study, and the p12R/K allele was lysine in Trovato's study, this stop codon does not appear to be associated with the p12R/K variation. Regarding the association with the termination codon immediately preceding the p12R/K variation and the *tax* subgroup, there were six HAM/TSP patients with *tax* B and one HAM/TSP patient with *tax* A. Thus, this termination codon immediately preceding the p12R/K variation was also not specifically associated with the *tax* subgroup.

To test whether HTLV-I having a *p12* sequence with either arginine (p12R) or lysine (p12K) at position 88 and HTLV-I with truncated $p12^{I}$ could persist stably over time, we compared the HTLV-I *p12* sequences at different time points. The observed *p12* nucleotide substitutions were the same in each person on each occasion (Table 3), suggesting that neither p12R/K nor a premature stop codon in $p12^{I}$ influences the course of HTLV-I infection. To examine whether HTLV-I with such a truncated $p12^{I}$ was transmissible, we further compared the *p12* sequence between HAM/TSP patients with a termination codon

TABLE 3. COMPARISON OF HTLV-I *p12* SEQUENCES AT DIFFERENT TIME POINTS WITH THE GRAND CONSENSUS SEQUENCE[a]

		Nucleotide change at position (amino acid position)					
	Date	*6900 (23)*	*6905 (24)*	*7078 (82)*	*7086 (85)*	*7093 (87)*	*7096 (88)*
Consensus		C (P)	T (P)	G (W)	C (L)	G (W)	G (R)
HAM 57	July 4, 1990				T (F)		G (R)
	August 29, 1997				T (F)		G (R)
HAM 70	June 27, 1990	T (S)	G (S)				G (R)
	February 27, 1998	T (S)	G (S)				G (R)
HAM 79	April 17, 1991						A (K)
	October 11, 2000						A (K)
HAM 105	March 11, 1992					A (Stop)	G (R)
	July 12, 2001					A (Stop)	G (R)
HAM 181	March 27, 1991			A (Stop)			G (R)
	January 15, 2000			A (Stop)			G (R)

[a]Amino acid of $p12^{I}$ is shown in parentheses.

TABLE 4. COMPARISON OF HTLV-I *p12* SEQUENCES WITHIN PEDIGREE WITH THE GRAND CONSENSUS SEQUENCE[a]

		Nucleotide change at position (amino acid change at position)						
	Sex	*6836 (1)*	*6840 (3)*	*6900 (23)*	*6905 (24)*	*7078 (82)*	*7094 (87)*	*7134*
Consensus		G (M)	T (L)	C (P)	T (P)	G (W)	G (W)	G
HAM 181	F					A (Stop)		
Husband of HAM 181	M					A (Stop)		
HAM 201	M		C (L)	T (S)	G (S)		A (Stop)	C
Wife of HAM 201	F		C (L)	T (S)	G (S)		A (Stop)	C
HAM 790	F						A (Stop)	
Sister of HAM 790	F						A (Stop)	
Mother of HAM 790	F						A (Stop)	
HAM 271	F	A (I)						
Sister of HAM 271 (AC)	F	A (I)						
Sister of HAM 271 (HAM)	F	A (I)						

[a]In the HAM 271 family, one sister was an asymptomatic HTLV-I carrier [HAM 271 (AC)] and one other sister was an HAM/TSP patient [HAM 271 (HAM)]. These three cases had an identical *p12* sequence with a destroyed initiation codon in the *p12* gene. Amino acid of $p12^I$ is shown in parentheses.

in the *p12* gene and their family members infected with HTLV-I. Interestingly, the *p12* sequences with a premature stop codon at either position 82 and 87 in HAM/TSP patients were identical in asymptomatic family members of HAM/TSP patients in each family. These findings also suggest that truncations of $p12^I$ at position 82 or 87 do not influence the infectivity of HTLV-I, although it was possible that the truncated $p12^I$ retained its function. However, in our study there was an HAM/TSP patient (HAM 271) with $p12^I$ in whom the $p12^I$ initiation codon was destroyed. In this case, the nucleotide at position 6836 had a substitution from G to A, changing the initiation codon ATG to ATA. We were interested to determine whether such a p12 with a destroyed initiation codon was transmissible in the patient's family. We examined HTLV-I sequences from two other HTLV-I-infected sisters in this family. One of the sisters was an HAM/TSP patient, while the other was an AC. The *p12* sequences were identical among these three sisters, with the same substitution at nt 6836 ($G \rightarrow A$) that destroyed the initiation codon of *p12*. This observation indicates that the destroyed *p12* was not a *de novo* mutation that happened in patient HAM 271, but rather was transmitted from their mother to the three sisters in this family. This contrasts with the observation that a putative immune escape mutation in the *tax* gene was observed in an ATL patient but not in the respective consensus sequence of asymptomatic HTLV-I carriers in the same family.[28] These findings strongly suggest that HTLV-I $p12^I$ is dispensable for HTLV-I transmission and the maintenance of HTLV-I infection. Regarding the relation between sequence variations in the HTLV-I *p12* gene and their association with HTLV-I-related diseases, lysine at position 88 (p12K) itself was not frequently observed in HAM/TSP patients (2 out of 144 HAM/TSP patients; 1.4%). However, the p12K variant, premature stop codons, and the destruction of the initiation codon were observed in 11 patients out of 144 HAM/TSP patients (7.4%), whereas none of these variations was observed in ACs. These variations in the *p12* gene may reduce the function of $p12^I$. Because p12K has a shorter life compared to p12R, and a premature stop codon in the $p12^I$ may reduce its function, the destruction of the initiation codon in the *p12* gene presumably ablates the function of $p12^I$. At the beginning of this study, we expected that alterations that reduce the function of the $p12^I$ would be less frequent in HAM/TSP, because HAM/TSP patients usually have a higher provirus load than ACs, and $p12^I$ had been suggested to confer a proliferative effect on HTLV-I-infected cells in an *in vitro* study. It is possible that the effects of $p12^I$ *in vivo* differ from its effects *in vitro*. However, the observed difference between HAM/TSP patients and ACs in the prevalence of these alterations that may reduce the function of $p12^I$ did not reach statistical significance, and it is therefore premature to conclude that mutations of the *p12* gene are implicated in the pathogenesis of HTLV-I-associated diseases. Further study with a larger number of ACs is necessary to clarify this point.

SEQUENCE DATA

DDBJ accession numbers: The accession numbers of the pX sequence including the entire *p12* gene in HAM/TSP cases are successively from AB127436 through AB127579. The accession numbers of the pX sequence including the entire *p12* gene in ATL cases are successively from AB154777 through AB154817. The accession numbers of the pX sequence including the entire *p12* gene in ACs are successively from AB158146 through AB158191. The accession numbers of the pX sequence including the entire *p12* gene at different occasions in Table 3 are AB127439 for HAM 57 at July 4, 1990, AB158267 for HAM 57 at August 29, 1997, AB127442 for HAM 70 at June 27, 1990, AB158266 for HAM 70 at February 27, 1998, AB127447 for HAM 79 at April 17, 1991,

AB158268 for HAM 79 at October 11, 2000, AB127458 for HAM 105 at March 11, 1992 and AB158270 for HAM 105 at July 12, 2001, AB127485 for HAM 181 at March 27, 1991 and AB158269 for HAM 181 at January 15, 2000. The accession numbers of the pX sequence including the entire *p12* gene of HAM/TSP patients and family members in Table 4 are AB127485 for HAM 181, AB158271 for the husband of HAM 181, AB127493 for HAM 201, AB158272 for the wife of HAM 201, AB127521 for HAM 271, AB158275 for the asymptomatic sister of HAM 271, AB158276 for the HAM/TSP sister of HAM 271, AB127562 for HAM 790, AB158273 for the sister of HAM 790, and AB158274 for the mother of HAM 790.

ACKNOWLEDGMENTS

This study was supported by in part from Takeda Science Foundation. We thank Ms. T. Muramoto and Ms. Y. Nishino (Department of Neurology and Geriatrics, Kagoshima University, Japan) for their excellent technical assistance. We also thank Professor Charles R.M. Bangham (Immunology Department, Imperial College Faculty of Medicine, United Kingdom) for critical reading of the manuscript. Presented in part at the 45th Conference Annual Meeting of the Japanese Society of Haematology, Nagoya, Japan, 29–31 August 2003. Informed consent was obtained from all HTLV-I carriers and patients. This research was approved by the institutional review boards of the author's institutions, and human experimentation guidelines of the U.S. Development of Health and Human Services and those of the author's institutions were followed in the conduct of clinical research. The authors have no commercial or other associations that might pose a conflict of interest.

REFERENCES

1. Poiesz BJ, Ruscetti FW, Gazdar AF, Bunn PA, Minna JD, and Gallo RC: Detection and isolation of type C retrovirus particles from fresh and cultured lymphocytes of a patient with cutaneous T-cell lymphoma. Proc Natl Acad Sci USA 1980;77:7415–7419.
2. Yoshida M, Miyoshi I, and Hinuma Y: Isolation and characterization of retrovirus from cell lines of human adult T-cell leukemia and its implication in the disease. Proc Natl Acad Sci USA 1982;79:2031–2035.
3. Gessain A, Barin F, Vernant JC, *et al.*: Antibodies to human T-lymphotropic virus type-I in patients with tropical spastic paraparesis. Lancet 1985;2:407–410.
4. Osame M, Usuku K, Izumo S, *et al.*: HTLV-I associated myelopathy, a new clinical entity. Lancet 1986;1:1031–1032.
5. Tajima K: The 4th nation-wide study of adult T-cell leukemia/lymphoma (ATL) in Japan: Estimates of risk of ATL and its geographical and clinical features. The T- and B-cell Malignancy Study Group. Int J Cancer 1990;45:237–243.
6. Kaplan JE, Osame M, Kubota H, *et al.*: The risk of development of HTLV-I-associated myelopathy/tropical spastic paraparesis among persons infected with HTLV-I. J Acquir Immune Defic Syndr 1990;3:1096–1101.
7. Daenke S, Nightingale S, Cruickshank JK, and Bangham CR: Sequence variants of human T-cell lymphotropic virus type I from patients with tropical spastic paraparesis and adult T-cell leukemia do not distinguish neurological from leukemic isolates. J Virol 1990;64:1278–1282.
8. Furukawa Y, Yamashita M, Usuku K, Izumo S, Nakagawa M, and Osame M: Phylogenetic subgroups of human T cell lymphotropic virus (HTLV) type I in the tax gene and their association with different risks for HTLV-I-associated myelopathy/tropical spastic paraparesis. J Infect Dis 2000;182:1343–1349
9. Giebler HA, Loring JE, van Orden K, *et al.*: Anchoring of CREB binding protein to the human T-cell leukemia virus type 1 promoter: A molecular mechanism of Tax transactivation. Mol Cell Biol 1997;17:5156–5164.
10. Siekevitz M, Feinberg MB, Holbrook N, Wong-Staal F, and Greene WC: Activation of interleukin 2 and interleukin 2 receptor (Tac) promoter expression by the trans-activator (tat) gene product of human T-cell leukemia virus, type I. Proc Natl Acad Sci USA 1987;84:5389–5393.
11. Brown DA, Nelson FB, Reinherz EL, and Diamond DJ: The human interferon-gamma gene contains an inducible promoter that can be transactivated by tax I and II. Eur J Immunol 1991;21: 1879–1885.
12. Fujii M, Sassone-Corsi P, and Verma IM: c-fos promoter trans-activation by the tax1 protein of human T-cell leukemia virus type I. Proc Natl Acad Sci USA 1988;85:8526–8530.
13. Berneman ZN, Gartenhaus RB, Reitz MS Jr, *et al.*: Expression of alternatively spliced human T-lymphotropic virus type I pX mRNA in infected cell lines and in primary uncultured cells from patients with adult T-cell leukemia/lymphoma and healthy carriers. Proc Natl Acad Sci USA 1992;89:3005–3009.
14. Franchini G, Mulloy JC, Koralnik IJ, *et al.*: The human T-cell leukemia/lymphotropic virus type I p12I protein cooperates with the E5 oncoprotein of bovine papillomavirus in cell transformation and binds the 16-kilodalton subunit of the vacuolar H+ ATPase. J Virol 1993;67:7701–7704.
15. Mulloy JC, Crownley RW, Fullen J, Leonard WJ, and Franchini G: The human T-cell leukemia/lymphotropic virus type 1 p12I proteins bind the interleukin-2 receptor beta and gammac chains and affects their expression on the cell surface. J Virol 1996; 70:3599–3605.
16. Collins ND, Newbound GC, Albrecht B, Beard JL, Ratner L, and Lairmore MD: Selective ablation of human T-cell lymphotropic virus type 1 p12I reduces viral infectivity in vivo. Blood 1998;91:4701–4707.
17. Koralnik IJ, Fullen J, and Franchini G: The p12I, p13II, and p30II proteins encoded by human T-cell leukemia/lymphotropic virus type I open reading frames I and II are localized in three different cellular compartments. J Virol 1993;67:2360–2366.
18. Ding W, Albrecht B, Kelley RE, *et al.*: Human T-cell lymphotropic virus type 1 p12(I) expression increases cytoplasmic calcium to enhance the activation of nuclear factor of activated T cells. J Virol 2002;76:10374–10382.
19. Johnson JM, Nicot C, Fullen J, *et al.*: Free major histocompatibility complex class I heavy chain is preferentially targeted for degradation by human T-cell leukemia/lymphotropic virus type 1 p12(I) protein. J Virol 2001;75:6086–6094.
20. Nicot C, Mulloy JC, Ferrari MG, *et al.*: HTLV-1 p12(I) protein enhances STAT5 activation and decreases the interleukin-2 requirement for proliferation of primary human peripheral blood mononuclear cells. Blood 2001;98:823–829.
21. Trovato R, Mulloy JC, Johnson JM, Takemoto S, de Oliveira MP, and Franchini G: A lysine-to-arginine change found in natural alleles of the human T-cell lymphotropic/leukemia virus type 1 p12(I) protein greatly influences its stability. J Virol 1999;73:6460–6467.
22. Martins ML, Soares BC, Ribas JG, *et al.*: Frequency of p12K and p12R alleles of HTLV type 1 in HAM/TSP patients and in asymptomatic HTLV type 1 carriers. AIDS Res Hum Retroviruses 2002;18:899–902.
23. Osame M: HTLV. In: *Human Retrovirology* (Blattner W, ed.). Raven, New York, 1990, pp. 191–197.

24. Shimoyama M: Diagnostic criteria and classification of clinical subtypes of adult T-cell leukaemia-lymphoma. A report from the Lymphoma Study Group (1984–87). Br J Haematol 1991;79:428–437.
25. Furukawa Y, Kubota R, Eiraku N *et al.*: Human T-cell lymphotropic virus type I (HTLV-I) related clinical and laboratory findings in HTLV-I infected blood donors. J Acquir Immune Defic Syndr 2003;32:328–334.
26. Seiki M, Hattori S, Hirayama Y, and Yoshida M: Human adult T-cell leukemia virus: Complete nucleotide sequence of the provirus genome integrated in leukemia cell DNA. Proc Natl Acad Sci USA 1983; 80:3618–3622.
27. Nagai M, Usuku K, Matsumoto W, *et al.*: Analysis of HTLV-I proviral load in 202 HAM/TSP patients and 243 asymptomatic HTLV-I carriers: High proviral load strongly predisposes to HAM/TSP. J Neurovirol 1998;4:586–593.
28. Furukawa Y, Kubota R, Tara M, Izumo S, and Osame M: Existence of escape mutant in HTLV-I tax during the development of adult T-cell leukemia. Blood 2001;97:987–993.

Address reprint requests to:
Yoshitaka Furukawa
Division of Blood Transfusion Medicine
Kagoshima University Hospital
8-35-1 Sakuragaoka
Kagoshima 890-8520, Japan

E-mail: furukawy@m2.kufm.kagoshima-u.ac.jp

Available online at www.sciencedirect.com
SCIENCE DIRECT®
Tetrahedron Letters
Tetrahedron Letters 45 (2004) 3651–3654

A new polymer-supported Evans-type chiral auxiliary derived from α-hydroxy-β-amino acid, phenylnorstatine: synthesis and application in solid-phase asymmetric alkylation reactions

Tomoya Kotake, S. Rajesh, Yoshio Hayashi, Yoshie Mukai, Mitsuhiro Ueda, Tooru Kimura and Yoshiaki Kiso*

Department of Medicinal Chemistry, Center for Frontier Research in Medicinal Science, Kyoto Pharmaceutical University, Yamashina-ku, Kyoto 607-8412, Japan

Received 6 February 2004; revised 2 March 2004; accepted 5 March 2004

Abstract—Based on a new anchoring strategy, a polymer-supported chiral oxazolidinone was prepared starting from (2*R*,3*S*)-3-amino-2-hydroxy-4-phenylbutanoic acid (phenylnorstatine, Pns) and Wang resin. Solid-phase asymmetric alkylation on this resin proceeded in high diastereoselectivity comparable to that of conventional solution-phase model experiments. This study suggests that anchoring through the 5-position of oxazolidinone is highly suited to achieving diastereoselective alkylation reactions on solid-support.

Recently, solid-phase organic synthesis has become a popular methodology for the preparation of organic molecules,[1] especially the preparation of compound libraries in the process of drug discovery.[2] It allows for a facile isolation of the desired compounds with easy elimination of by-products and excess reagents using a full- or semi-automatic process. Polymer-supported chiral auxiliaries are especially advantageous because they can be recovered by simple filtration and potentially recycled. Evans' oxazolidinone is one of the most versatile chiral auxiliaries for asymmetric acyl group-based transformation.[3] The attachment of Evans' oxazolidinone to solid-supports and its utility in asymmetric alkylation,[4] aldol condensation,[5] and Diels–Alder,[6] and 1,3-dipolar[7] cycloadditions have been reported using **1** (Fig. 1A). However, the application of **1** is limited, probably due to the difficulty of monitoring and optimizing the solid-phase reaction more than the corresponding solution-phase reactions. In addition, the solid-phase asymmetric alkylation on the resin **1** has not been accomplished in a high stereoselective manner (max 90% ee) and a marked undesired effect of the solid-supports on the yield and ee was reported.[4] One reason for these undesired results could be that the critical chiral discriminating unit, that is, the benzyl group at

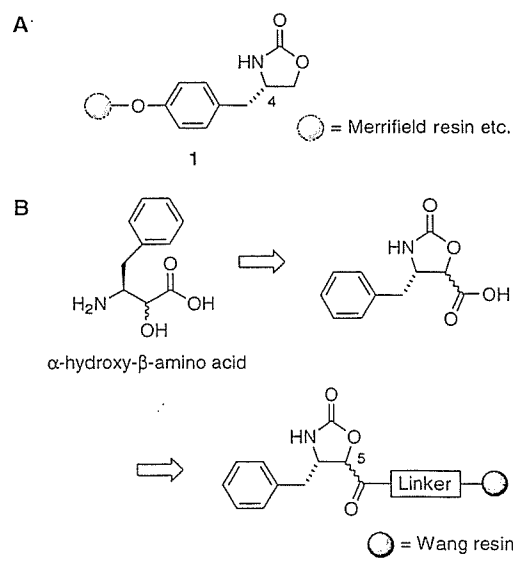

Figure 1. Polymer-supported Evans-type chiral auxiliaries. (A) Chiral auxiliary anchored at the 4-position.[4–7] (B) The new auxiliary derived from α-hydroxy-β-amino acid anchored at the 5-position.

Keywords: Evans' oxazolidinone; Chiral auxiliary; Phenylnorstatine; Asymmetric alkylation; Solid-phase; Polymer-supported.
* Corresponding author. Tel.: +81-75-595-4635; fax: +81-75-591-9900; e-mail: kiso@mb.kyoto-phu.ac.jp

0040-4039/$ - see front matter © 2004 Elsevier Ltd. All rights reserved.
doi:10.1016/j.tetlet.2004.03.043

the 4-position of the oxazolidinone ring in **1**, was used to anchor the solid-support.

Hence, to create a new anchor liberating the benzyl group, we focused on the chiral α-hydroxy-β-amino acids, phenylnorstatine [Pns, (2*R*,3*S*)-3-amino-2-hydroxy-4-phenylbutanoic acid] and its (2*S*,3*S*)-stereoisomer, allophenylnorstatine (Apns), which are well-known units with the hydroxymethylcarbonyl (HMC) isostere necessary for inhibiting aspartyl proteases.[8] As shown in Figure 1B, these α-hydroxy-β-amino acids can be converted to the corresponding oxazolidinones with a carboxyl group at the 5-position of the ring for anchoring to the solid-support. Here, we describe the synthesis of a new polymer-supported Evans' chiral auxiliary derived from Pns and demonstrate that solid-phase asymmetric alkylation proceeds with high stereoselectivity parallel to that obtained with the model substrate under classical solution conditions.

In the design of new polymer-supported oxazolidinone, piperidine-4-carboxylic acid was used as a linker, which can connect the chiral auxiliary through a base-insensitive tertiary-amide bond. Wang resin[9] was used as the solid-support, since the ester bond between the linker and resin can be easily formed by standard condensation methods and cleaved by mild acids like TFA or methanolysis to monitor the reaction.

The synthesis of oxazolidinone derivative **4** is outlined below (Scheme 1). Boc—Pns—OH[10] **2** was coupled to benzyl piperidine-4-carboxylate·HCl by the EDC–HOBt method[11] to give **3**. Removal of the *N*-Boc group of **3** and subsequent reaction with 1,1′-carbonyldiimidazole (CDI)[12] gave the desired oxazolidinone **4** in good yields.[13] During this cyclization reaction, no epimerization at the 5-position, and no aziridine by-product formation[14] were observed. Oxazolidinone **4** was then *N*-3-phenylpropionylated and the resultant carboximide **5a** was subjected to a model alkylation study in the solution-phase.[15] As Table 1 shows, the new oxazolidinone derivative **4** could function as an efficient chiral auxiliary with suitable reactivity in terms of yield and stereoselectivity. In addition, no disruption of both the oxazolidinone ring and the benzyl ester was observed during the cleavage with LiOOH.[16] Similar results were also obtained in the use of other imides **5b** and **5c** with *N*-phenoxyacetyl and *N*-propionyl groups, respectively (Table 1).

In the case of *N*-acyloxazolidinone derived from Boc—Apns—OH, epimerization at the 5-position was observed during the base treatment, suggesting that the 5-position as well as the desired α-position of the acyl group were deprotonated by LDA, while deprotonation in the Pns-derived *N*-acyloxazolidinone was specific to the α-position. This was probably due to increased acidity at

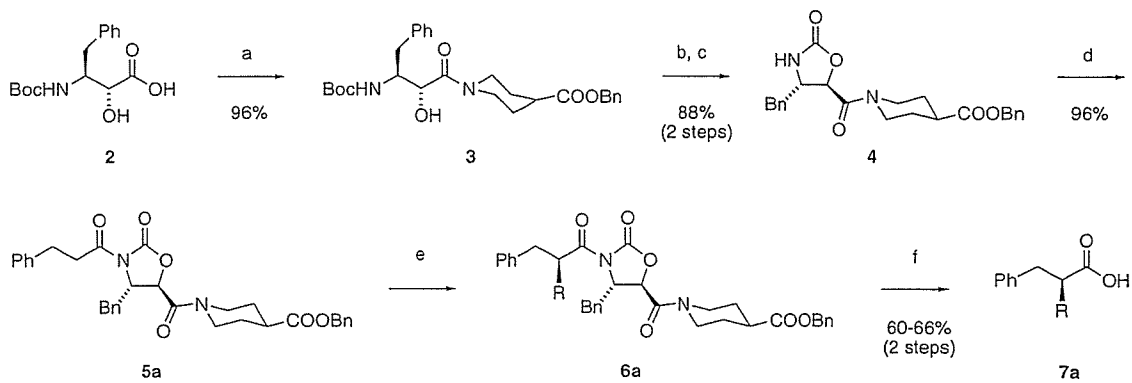

Scheme 1. Reagents and conditions: (a) benzyl piperidine-4-carboxylate·HCl, HOBt·H_2O, EDC·HCl, Et_3N, DMF, 0 °C to rt; (b) 4 M HCl/1,4-dioxane, 0 °C to rt; (c) Et_3N, CDI, THF, 0 °C to rt; (d) 3-phenylpropionic acid, ^{t}BuCOCl, Et_3N, LiCl, THF, −18 °C to rt; (e) LDA, RX, THF, −78 to 0 °C; (f) LiOH, 30% H_2O_2, THF–H_2O (3:1), 0 °C.

Table 1. Results of asymmetric alkylation

Entry	Imide	R^2X	Solid-phase		Solution-phase	
			Yield (%)[a]	Ee (%)[b]	Yield (%)[c]	Ee (%)[b]
1	**10**/**5a**	MeI	48	85	62	86
2	**10**/**5a**		54	96	66	96
3	**10**/**5a**		51	94	64	95
4	**10**/**5a**		47	92	60	90
5	**11**/**5b**		38	96	48	96
6	**12**/**5c**	BnBr	40	97	57	98

[a] Yield in four steps based on original loading of Wang resin (see Scheme 2).
[b] Determined by HPLC analysis after conversion to the corresponding (*S*)-phenylethyl amide derivatives.
[c] Yield in two steps starting from **5** (see Scheme 1).

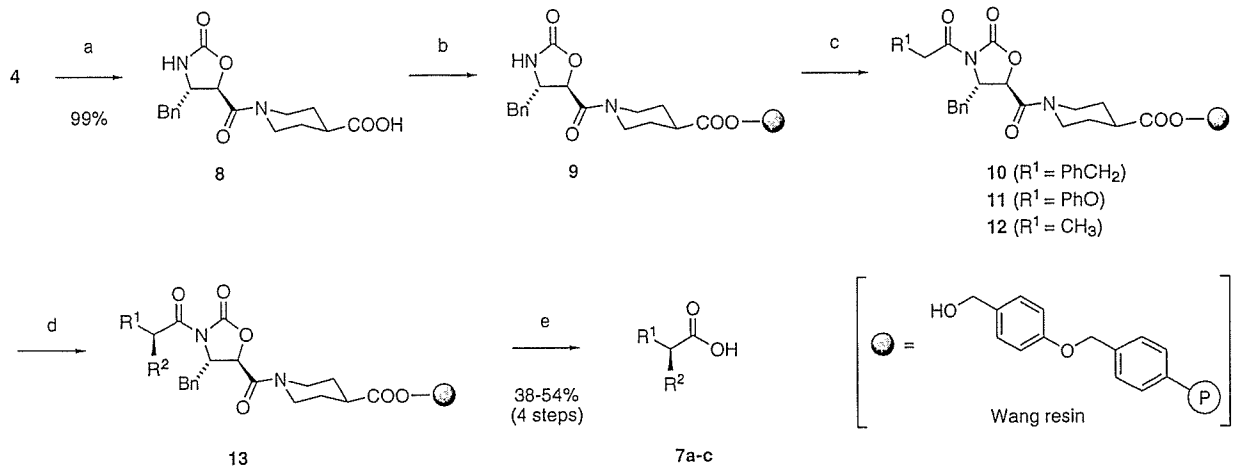

Scheme 2. Reagents and conditions: (a) H_2, Pd/C, MeOH–H_2O (9:1), rt, overnight; (b) Wang resin, DIC, DMAP, DMF, rt, 3 h; (c) $R^1CH_2CO_2H$, 2-chloro-1-methylpyridinium iodide, Et_3N, DMAP, CH_2Cl_2, rt, 2 h; (d) LDA, R^2X, THF, 0 °C, 3.5 h; (e) LiOH, 30% H_2O_2, THF–H_2O (3:1), 0 °C, 1 h.

the 5-position of the Apns-derived oxazolidinone caused by steric repulsion between the benzyl and carboxamide groups in a *cis*-configuration.

Hence, for the solid-phase synthesis, Pns-derived oxazolidinone **4** was selected and its benzyl ester was removed by hydrogenolysis, and the resultant carboxylic acid **8** was attached to the Wang resin by the established method with 1,3-diisopropylcarbodiimide (DIC)[17] in the presence of a catalytic amount of DMAP (Scheme 2). Analysis of the loading rate by methanolysis of the resin **9** gave a complete recovery of the corresponding methyl ester, indicating that quantitative loading was achieved. It is pertinent to note that the previous reported auxiliary **1** on Wang resin having only 56% of loading might have potential side reactions by the residual free-hydroxyl group.[4] On the contrary, we were able to efficiently synthesize a new Wang resin-supported Evans-type chiral auxiliary **9** with a quantitative loading.

For the solid-phase asymmetric alkylation, to a well-swollen carboximide resin **10–12** in THF, derived from **9** by the mixed anhydride-LiCl N-acylation[18] or Mukaiyama reagent,[19] was added LDA (2 equiv) at 0 °C, followed by the addition of alkyl halide (10 equiv). After stirring for 3 h at the same temperature, the solid-phase reaction was quenched by adding saturated aqueous NH_4Cl. The resin was recovered by filtration and was subsequently washed with THF and MeOH to give **13**. LiOOH-mediated chemoselective hydrolysis of **13** gave the desired chiral α-alkylated carboxylic acids **7a–c**.[20] Since no disruption of the ester bond between the linker and resin was observed during these steps and methanolysis of recovered resin afforded the corresponding oxazolidinone methyl ester in high yield (94% yield Table 1, entry 2), it indicated that the polymer-supported auxiliary was stable to LiOOH treatment. Therefore, it is considered that the recovered resin **9** has a potential for reuse. Enantiomeric excess of the obtained acids was determined by HPLC analysis after derivatization to the corresponding (*S*)-phenylethyl amides by the EDC–HOBt method. As Table 1 shows, high stereoselectivity (85–97% ee) comparable to the solution-phase model experiments was obtained in this solid-phase system with a total yield of 38–54% (in four steps), calculated from the original loading of Wang resin. These results suggest that anchoring to the resin at the 5-position of the oxazolidinone ring is highly suitable for realizing reasonable enantiomeric ratios, probably achieving greater freedom from the polystyrene scaffold than the previous auxiliary involving the 4-position. It also suggests that the asymmetric alkylation reaction proceeded through the same chelation controlled model as reported in standard Evans-type oxazolidinone chemistry.[3a] These findings would resolve the concern raised by Burgess and Lim[4] in the solid-phase asymmetric alkylation using the polymer-supported Evans' chiral auxiliary, and our new polymer-supported oxazolidinone is applicable in the synthesis of a variety of chiral α-alkylated carboxylic acids.

In conclusion, we have developed a new polymer-supported Evans-type chiral auxiliary, anchored to the Wang resin through a carboxyl group at the 5-position of the oxazolidinone ring and a piperidine-4-carboxyl linker, and found it to be a useful tool for solid-phase asymmetric alkylation with no reduction in stereoselectivity. This convenient polymer-supported chiral auxiliary is applicable in the preparation of a library of chiral α-branched carboxylic acids such as 3-phenylpropionic acid derivatives having inhibitory activity against serine proteases.[21] Further studies of well-known asymmetric reactions in the use of the Evans' auxiliary, such as aldol condensation and cycloadditions, and the recycling of the resin are under investigation.

Acknowledgements

This research was supported in part by grants and the Frontier Research Program of the Ministry of Education, Science and Culture of Japan.

References and notes

1. (a) Seneci, P. *Solid Phase and Combinatorial Technologies*; John Wiley & Sons: New York, 2000; (b) Obrecht, D.; Villalgordo, J. M. In *Solid-Supported Combinatorial and Parallel Synthesis of Small Molecular-Weight Compound Libraries. Tetrahedron Organic Chemistry Series*; Elsevier: Oxford, 1998; Vol. 17.
2. (a) Geysen, H. M.; Schoenen, F.; Wagner, D.; Wagner, R. *Nat. Rev. Drug Discovery* **2003**, *2*, 222–230; (b) Gallop, M. A.; Barrett, R. W.; Dower, W. J.; Fodor, S. P. A.; Gordon, E. M. *J. Med. Chem.* **1994**, *37*, 1233–1251.
3. (a) Evans, D. A. *Aldrichim. Acta* **1982**, *15*, 23–32; (b) Ager, D. J.; Prakash, I.; Schaad, D. R. *Aldrichim. Acta* **1997**, *30*, 3–11.
4. Burgess, K.; Lim, D. *Chem. Commun.* **1997**, 785–786.
5. (a) Purandare, A. V.; Natarajan, S. *Tetrahedron Lett.* **1997**, *38*, 8777–8780; (b) Phoon, C. W.; Abell, C. *Tetrahedron Lett.* **1998**, *39*, 2655–2658.
6. Winkler, J. D.; McCoull, W. *Tetrahedron Lett.* **1998**, *39*, 4935–4936.
7. (a) Faita, G.; Paio, A.; Quadrelli, P.; Rancati, F.; Seneci, P. *Tetrahedron Lett.* **2000**, *41*, 1265–1269; (b) Faita, G.; Paio, A.; Quadrelli, P.; Rancati, F.; Seneci, P. *Tetrahedron* **2001**, *57*, 8313–8322; (c) Desimoni, G.; Faita, G.; Galbiati, A.; Pasini, D.; Quadrelli, P.; Rancati, F. *Tetrahedron: Asymmetry* **2002**, *13*, 333–337.
8. (a) Mimoto, T.; Kato, R.; Takaku, H.; Nojima, S.; Terashima, K.; Misawa, S.; Fukazawa, T.; Ueno, T.; Sato, H.; Shintani, M.; Kiso, Y.; Hayashi, H. *J. Med. Chem.* **1999**, *42*, 1789–1802; (b) Mimoto, T.; Hattori, N.; Takaku, H.; Kisanuki, S.; Fukazawa, T.; Terashima, K.; Kato, R.; Nojima, S.; Misawa, S.; Ueno, T.; Imai, J.; Enomoto, H.; Tanaka, S.; Sakikawa, H.; Shintani, M.; Hayashi, H.; Kiso, Y. *Chem. Pharm. Bull.* **2000**, *48*, 1310–1326.
9. Wang resin was purchased from Watanabe Chem. Ind., Ltd (Hiroshima, Japan), loading 0.75 mmol/g, 100–200 mesh, polystyrene with 1% cross linking with divinylbenzene.
10. Boc—Pns—OH was prepared from H—Pns—OH, which was purchased from Nippon Kayaku (Tokyo, Japan).
11. König, W.; Geiger, R. *Chem. Ber.* **1970**, *103*, 788–798.
12. Bunnage, M. E.; Davies, S. G.; Goodwin, C. J.; Ichihara, O. *Tetrahedron* **1994**, *50*, 3975–3986.
13. Chemical data for benzyl *N*-[(4*S*)-benzyl-1,3-oxazolidin-2-one-5-carbonyl]piperidine-4-carboxylate (**4**): mp 91–93 °C; R_f 0.55 (*n*-hexane:AcOEt = 1:5); ^{1}H NMR (300 MHz, $CDCl_3$) δ 7.20–7.40 (m, 10H), 5.25 (br s, 1H), 5.14 (s, 1H), 5.12 (s, 1H), 4.79 (d, 0.5H, J = 5.5 Hz), 4.78 (d, 0.5H, J = 5.5 Hz), 4.63–4.69 (m, 1H), 4.33–4.38 (m, 0.5H), 4.16–4.20 (m, 0.5H), 3.80–3.84 (m, 0.5H), 3.65–3.70 (m, 0.5H), 3.14–3.24 (m, 0.5H), 2.93–3.02 (m, 2H), 2.76–2.88 (m, 1.5H), 2.54–2.65 (m, 1H), 1.55–1.98 (m, 4H); ^{13}C NMR (75.5 MHz, $CDCl_3$) δ 173.7, 173.4, 164.4, 164.3, 156.9, 135.8, 135.8, 135.7, 129.1, 129.0, 128.6, 128.3, 128.3, 128.1, 127.3, 76.8, 76.6, 66.5, 55.3, 44.8, 44.5, 42.0, 41.8, 41.0, 41.0, 40.9, 40.3, 28.4, 28.2, 27.5, 27.5; $[\alpha]_D^{27}$ −91.2 (c 1.281, $CHCl_3$); IR (KBr) 3452, 3036, 3007, 1771, 1730, 1653, 1456, 1387, 1313, 1271, 1238, 1209, 1173, 1038, 1011, 756, 737, 698, 667 cm^{-1}; HRMS (EI$^+$): m/z 422.1845 for [M$^+$] (calcd 422.1842 for $C_{24}H_{26}N_2O_5$); elemental analysis calcd for $C_{24}H_{26}N_2O_5$: C, 68.23; H, 6.20; N, 6.63. Found: C, 67.99; H, 6.20; N, 6.55.
14. Cutugno, S.; Martelli, G.; Negro, L.; Savoia, D. *Eur. J. Org. Chem.* **2001**, 517–522.
15. General procedure for solution-phase chiral synthesis of α-alkylated carboxylic acids using compound **5**: Briefly, to a solution of **5** in THF, was added LDA (1.2 equiv) dropwise at −78 °C. After stirring for 30 min, the solution was quenched with the alkyl halide (10 equiv), and warmed to 0 °C in 3 h with stirring. Stirring again with saturated NH_4Cl solution followed by the extraction with AcOEt, washing the organic layer with water and brine, drying over Na_2SO_4, and finally the removal of the solvent gave **6**. Without further purification, the LiOOH hydrolysis of **6** was carried out according to the previous report,[16] and then the product was purified by preparative TLC for removing nonalkylated carboxylic acid. The resultant pure **7** was next coupled with (*S*)-phenylethylamine by the EDC–HOBt method to determine the enantiomeric excesses of the α-alkylated carboxylic acids **7** by HPLC.
16. (a) Evans, D. A.; Britton, T. C.; Ellman, J. A. *Tetrahedron Lett.* **1987**, *28*, 6141–6144; (b) Evans, D. A.; Ellman, J. A. *J. Am. Chem. Soc.* **1989**, *111*, 1063–1072.
17. Atherton, E.; Benoiton, N. L.; Brown, E.; Sheppard, R. C.; Williams, B. J. *J. Chem. Soc., Chem. Commun.* **1981**, 336–337.
18. Ho, G.-J.; Mathre, D. J. *J. Org. Chem.* **1995**, *60*, 2271–2273.
19. Mukaiyama, T. *Angew. Chem., Int. Ed. Engl.* **1979**, *18*, 707–721.
20. The crude product **7** was purified by preparative TLC to remove nonalkylated carboxylic acid. The relatively lower yield (38–54%) that was observed in the solid-phase method was due to the fact that the yield includes the four step reaction from Wang resin to the final product **7**. The yield for two steps (alkylation and hydrolysis) is likely to be similar to that of the solution-phase method.
21. Kim, D. H.; Li, Z.-H.; Lee, S. S.; Park, J.; Chung, S. J. *Bioorg. Med. Chem.* **1998**, *6*, 239–249.

PROTEINS: Structure, Function, and Bioinformatics 55:594–602 (2004)

A Structural and Thermodynamic Escape Mechanism from a Drug Resistant Mutation of the HIV-1 Protease

Sonia Vega,[1†] Lin-Woo Kang,[2†] Adrian Velazquez-Campoy,[1] Yoshiaki Kiso,[3] L. Mario Amzel,[2] and Ernesto Freire[1*]
[1]*Department of Biology, The Johns Hopkins University, Baltimore, MD 21218*
[2]*Department of Biophysics and Biophysical Chemistry, The Johns Hopkins University School of Medicine, Baltimore, MD 21218*
[3]*Department of Medicinal Chemistry, Center for Frontier Research in Medicinal Science, Kyoto Pharmaceutical University, Yamashina-ku, Kyoto 607-8412, Japan*

ABSTRACT **The efficacy of HIV-1 protease inhibition therapies is often compromised by the appearance of mutations in the protease molecule that lower the binding affinity of inhibitors while maintaining viable catalytic activity and substrate affinity. The V82F/I84V double mutation is located within the binding site cavity and affects all protease inhibitors in clinical use. KNI-764, a second-generation inhibitor currently under development, maintains significant potency against this mutation by entropically compensating for enthalpic losses, thus minimizing the loss in binding affinity. KNI-577 differs from KNI-764 by a single functional group critical to the inhibitor response to the protease mutation. This single difference changes the response of the two inhibitors to the mutation by one order of magnitude. Accordingly, a structural understanding of the inhibitor response will provide important guidelines for the design of inhibitors that are less susceptible to mutations conveying drug resistance. The structures of the two compounds bound to the wild type and V82F/I84V HIV-1 protease have been determined by X-ray crystallography at 2.0 Å resolution. The presence of two asymmetric functional groups, linked by rotatable bonds to the inhibitor scaffold, allows KNI-764 to adapt to the mutated binding site cavity more readily than KNI-577, with a single asymmetric group. Both inhibitors lose about 2.5 kcal/mol in binding enthalpy when facing the drug-resistant mutant protease; however KNI-764 gains binding entropy while KNI-577 loses binding entropy. The gain in binding entropy by KNI-764 accounts for its low susceptibility to the drug-resistant mutation. The heat capacity change associated with binding becomes more negative when KNI-764 binds to the mutant protease, consistent with increased desolvation. With KNI-577, the opposite effect is observed. Structurally, the crystallographic B factors increase for KNI-764 when it is bound to the drug-resistant mutant. The opposite is observed for KNI-577. Consistent with these observations, it appears that KNI-764 is able to gain binding entropy by a two-fold mechanism: it gains solvation entropy by burying itself deeper within the binding pocket and gains conformational entropy by losing interaction with the protease. Proteins 2004;55:594–602.**

Key words: HIV protease; drug resistance; thermodynamics; crystallography; calorimetry

INTRODUCTION

A significant obstacle to the efficacy of drugs directed against viral targets is the appearance of drug-resistant mutations in the targeted molecules. The clinical use of HIV-1 protease inhibitors in antiretroviral therapies clearly illustrates the capacity of the virus to mutate and develop strains carrying mutant protease molecules with a significantly lower affinity for the inhibitors while maintaining sufficient catalytic activity for viral reproduction.[1–9] To be effective against a wide spectrum of protease variants, an inhibitor needs to exhibit an extremely high activity against wild-type protease and be affected only mildly by protease mutations. Ideally, an inhibitor should have a binding affinity in the 1–50 pM range against the wild type and be affected by mutations by a factor of 100 or less.[10–12] The extremely high activity required against the wild type can only be achieved if both enthalpy and entropy contribute favorably to the Gibbs energy.

In this article we describe the high resolution crystallographic structures of the complexes of two chemically and structurally similar HIV-1 protease inhibitors (KNI-764 and KNI-577) with the wild type HIV-1 protease and a common mutation associated with drug resistance to protease inhibitors currently in clinical use (V82F/I84V). Both inhibitors bind to the wild-type HIV-1 protease with high affinity but respond differently to the mutation.[10] Despite their chemical and structural similarities, KNI-577 loses binding affinity by a factor of 200 while KNI-764 loses binding affinity only by a factor of 20.[10] By combining high resolution structural data with binding thermodynamic results for both inhibitors against wild type and mutant protease, we attempt to understand the mechanism by

Grant sponsor: National Institutes of Health; Grant numbers: GM57144 (E.F.) and GM45540 (L.M.A.).

*Correspondence to: Ernesto Freire, Department of Biology, The Johns Hopkins University, 3400 North Charles, Baltimore, MD 21218, USA. Email: ef@jhu.edu.

†Sonia Vega and Lin-Woo Kang contributed equally to this paper.

Received 18 August 2003; 3 November 2003; Accepted 18 November 2003

Published online 1 April 2004 in Wiley InterScience (www.interscience.wiley.com). DOI: 10.1002/prot.20069

which an inhibitor can evade the negative effects of mutations. This mechanism could delineate a general strategy for the design of drug molecules that are more resistant to the effect of target mutations.

METHODS

Protein Purification

Protease expression, purification and refolding were performed as described before.[25,26] Briefly, plasmid-encoded HIV-1 protease was expressed as inclusion bodies in *E. coli* BL21(DE3). Cells were suspended in extraction buffer (20 m*M* Tris, 1 m*M* EDTA, 10 m*M* 2-ME, pH 7.5) and broken with two passes through a French pressure cell (≥16000 psi). Cell-debris and protease-containing inclusion bodies were collected by centrifugation (20,000 g for 20 min at 4°C). Inclusion bodies were washed with three buffers. Each wash consisted of re-suspension (glass homogenizer, sonication) and centrifugation (20,000 g for 20 min at 4°C). In each step a different washing buffer was employed: buffer-1 (25 m*M* Tris, 2.5 m*M* EDTA, 0.5*M* NaCl, 1 m*M* Gly-Gly, 50 m*M* 2-ME, pH 7.0); buffer-2 (25 m*M* Tris, 2.5 m*M* EDTA, 0.5*M* NaCl, 1 m*M* Gly-Gly, 50 m*M* 2-ME, 1*M* urea, pH 7.0); buffer-3 (25 m*M* Tris, 1 m*M* EDTA, 1 m*M* Gly-Gly, 50 m*M* 2-ME, pH 7.0). Protease was solubilized in 25 m*M* Tris, 1 m*M* EDTA, 5 m*M* NaCl, 1 m*M* Gly-Gly, 50 m*M* 2-ME, 9*M* urea, pH 9.0, clarified by centrifugation and applied directly to an anion exchange Q-Sepharose column (Q-Sepharose HP, Pharmacia) previously equilibrated with the same buffer. The protease was passed through the column and then acidified by adding formic acid to 25 m*M* immediately upon elution from the column. Precipitation of a significant amount of the contaminants occurred upon acidification. Protease-containing fractions were pooled, concentrated and stored at 4°C at 5–10 mg/mL.

The HIV-1 protease was folded by ten-fold stepwise dilution into 10 m*M* formic acid at 0°C. The pH was gradually increased to 3.8, and then the temperature was raised to 30°C. Sodium acetate (pH 5.0) was added to increase the pH to 5.0, and the protein was concentrated. Folded protease was desalted into 1 m*M* sodium acetate at pH 5.0 using a gel filtration column (PD-10, Pharmacia) and stored at either 4°C or −20°C (≥2.5 mg/ml) without loss of activity over several weeks. After folding, the protease was estimated to be ≥99% pure.

Activity of the refolded protein was assessed by active site titration, performed by isothermal titration calorimetry (VP-ITC, Microcal LLC, Northampton MA) as described before.[11,17]

Isothermal Titration Calorimetry

Isothermal titration calorimetry experiments were carried out using a high precision VP-ITC titration calorimetric system (Microcal Inc, Northampton, MA). The enzyme solution (10–20 μ*M* dimer) in the calorimetric cell was titrated with KNI-764, KNI-577 or acetyl-pepstatin (0.15-0.3 m*M*) dissolved in the same buffer (10 m*M*, DMSO 2% v/v). In displacement titration experiments (see below), inhibitors were injected into the calorimetric cell containing the protein pre-bound to a weak inhibitor (acetyl-pepstatin) as described before.[11,12,26] The concentration of acetyl-pepstatin in the titration cell was 0.2 m*M*. Protein and inhibitor solutions were properly degassed and carefully loaded into the cells to avoid bubble formation during stirring. Exhaustive cleaning of the cells was undertaken before each experiment. The heat evolved after each ligand injection was obtained from the integral of the calorimetric signal. The heat due to the binding reaction between the inhibitor and the enzyme was obtained as the difference between the heat of reaction and the corresponding heat of dilution. Blank experiments were performed by injecting the inhibitor into buffer solution to confirm the absence of self-association effects in the ligand.

The binding enthalpy was measured at two pH values (3.8 and 5.0) using several buffers differing in ionization enthalpy (acetate 0.12 kcal/mol, MES 3.72 kcal/mol, ACES 7.51 kcal/mol, cacodylate −0.47 kcal/mol, formate −0.05 kcal/mol, glycine 1.07 kcal/mol, cytidine 4.50 kcal/mol). The extension and contribution of protonation/deprotonation processes to the binding were assessed by determination of the pH-dependence of the binding enthalpy. The pH values were selected according to a previous work with KNI-272, another allophenylnorstatine-based inhibitor, which exhibits maximal and minimal proton release upon binding at these pH values.[17] The binding enthalpy of both KNI-764 and KNI-577 showed no dependence on the ionization enthalpy of the buffer, indicating no net proton exchange under the conditions of these experiments.

Displacement Isothermal Titration Calorimetry

KNI-764 and KNI-577 are tightly-binding inhibitors ($K_d < 1$ n*M*) of the HIV-1 protease, and therefore standard titration experiments do not provide accurate estimates of the binding affinity, even though the binding enthalpy can be determined with high accuracy. In order to overcome this impediment, calorimetric displacement titrations were carried out, allowing for the determination of the affinity and enthalpy of binding.[11,12,26,27] In calorimetric displacement titrations, the high-affinity inhibitor is titrated into a protease sample pre-bound to a weaker inhibitor. Under these conditions, the apparent binding affinity of the tight inhibitor diminishes in a manner proportional to the affinity and free concentration of the weak inhibitor and becomes calorimetrically measurable. Two calorimetric titrations are required to solve the binding equations and determine the binding affinity and binding enthalpy of the tightly-binding inhibitor: the titration of the weak inhibitor into the protease and the titration of the high-affinity inhibitor into the protease pre-bound to the weak inhibitor. Analysis of the data was performed using software developed in this laboratory as described previously.[11] The change in heat capacity, the temperature derivative of the binding enthalpy, was determined by performing titrations at different temperatures (Fig. 1). It can be calculated as the slope from the linear regression of binding enthalpy versus temperature.